LANGMUIR

pubs.acs.org/Langmuir Review

Structure of the Bacterial Cell Envelope and Interactions with Antimicrobials: Insights from Molecular Dynamics Simulations

Published as part of Langmuir virtual special issue "2023 Pioneers in Applied and Fundamental Interfacial Chemistry: Nicholas D. Spencer".

Pradyumn Sharma,[¶] Rakesh Vaiwala,[¶] Amar Krishna Gopinath, Rajalakshmi Chockalingam, and K. Ganapathy Ayappa*

Cite This: *Langmuir* 2024, 40, 7791−7811 Read Online

ACCESS | Metrics & More | Article Recommendations

ABSTRACT: Bacteria have evolved over 3 billion years, shaping our intrinsic and symbiotic coexistence with these single-celled organisms. With rising populations of drug-resistant strains, the search for novel antimicrobials is an ongoing area of research. Advances in high-performance computing platforms have led to a variety of molecular dynamics simulation strategies to study the interactions of antimicrobial molecules with different compartments of the bacterial cell envelope of both Gram-positive and Gram-negative species. In this review, we begin with a detailed description of the structural aspects of the bacterial cell envelope. Simulations concerned with the transport and associated free energy of small molecules and ions through the outer membrane, peptidoglycan, inner membrane and outer membrane porins are discussed. Since surfactants are widely used as antimicrobials, a section is devoted to the interactions of surfactants with the cell wall and inner membranes. The review ends with a discussion on antimicrobial peptides and the insights gained from the molecular simulations on the free energy of translocation. Challenges involved in developing accurate molecular models and coarse-grained strategies that provide a trade-off between atomic details with a gain in sampling time are highlighted. The need for efficient sampling strategies to obtain accurate free energies of translocation is also discussed. Molecular dynamics simulations have evolved as a powerful tool that can potentially be used to design and develop novel antimicrobials and strategies to effectively treat bacterial infections.

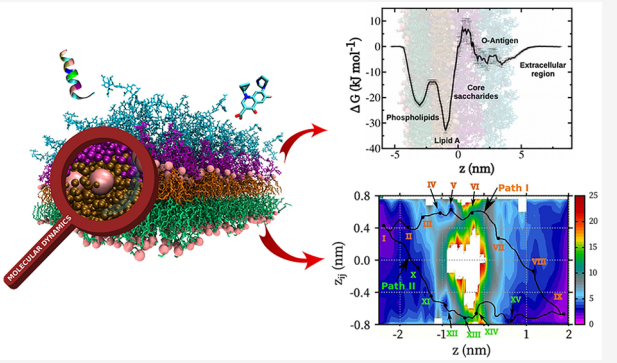

INTRODUCTION

Cells form the basic structural, functional, and biological units of all living organisms. Cell surfaces of bacteria and viruses have evolved complex and intricate mechanisms to support their lifeforms. Bacterial cell surfaces, which are the focus of this review, have a complex and layered landscape made up of proteins, lipids, and sugars designed to control cellular metabolic functions, cell division and offer protection from external threat. The semi-permeable cell envelope regulates the transport of various molecules, nutrients, and other metabolites.

Perhaps the most widely used strategy for combating bacterial infections involves the use of external agents or antimicrobials to directly target the bacterial cell envelope. Irrespective of the pathways taken to kill bacteria, these antimicrobial molecules first encounter and interact with the bacterial cell envelope to either disrupt the envelope[1] or access the cytoplasm in order to initiate bacteriostatic or bactericidal activity.[2] Although bacterial kill assays are widely used to assess the efficacy of antimicrobial molecules, the molecular mechanisms for cellular entry and subsequent interactions are poorly understood.

Developing models to study realistic representations of the cell envelope is an evolving area of research in both experiments and simulations.[3−5] Experimental techniques,[6−9] such as fluorescence correlation spectroscopy, single-particle tracking, X-ray scattering, mass spectroscopy, super-resolution single-molecule methods, and atomic force microscopy, have improved our molecular understanding of the structure and complexity of the bacterial cell surface.

Received: November 13, 2023
Revised: February 16, 2024
Accepted: February 19, 2024
Published: March 7, 2024

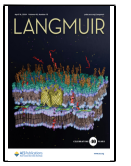

https://doi.org/10.1021/acs.langmuir.3c03474
Langmuir 2024, 40, 7791−7811

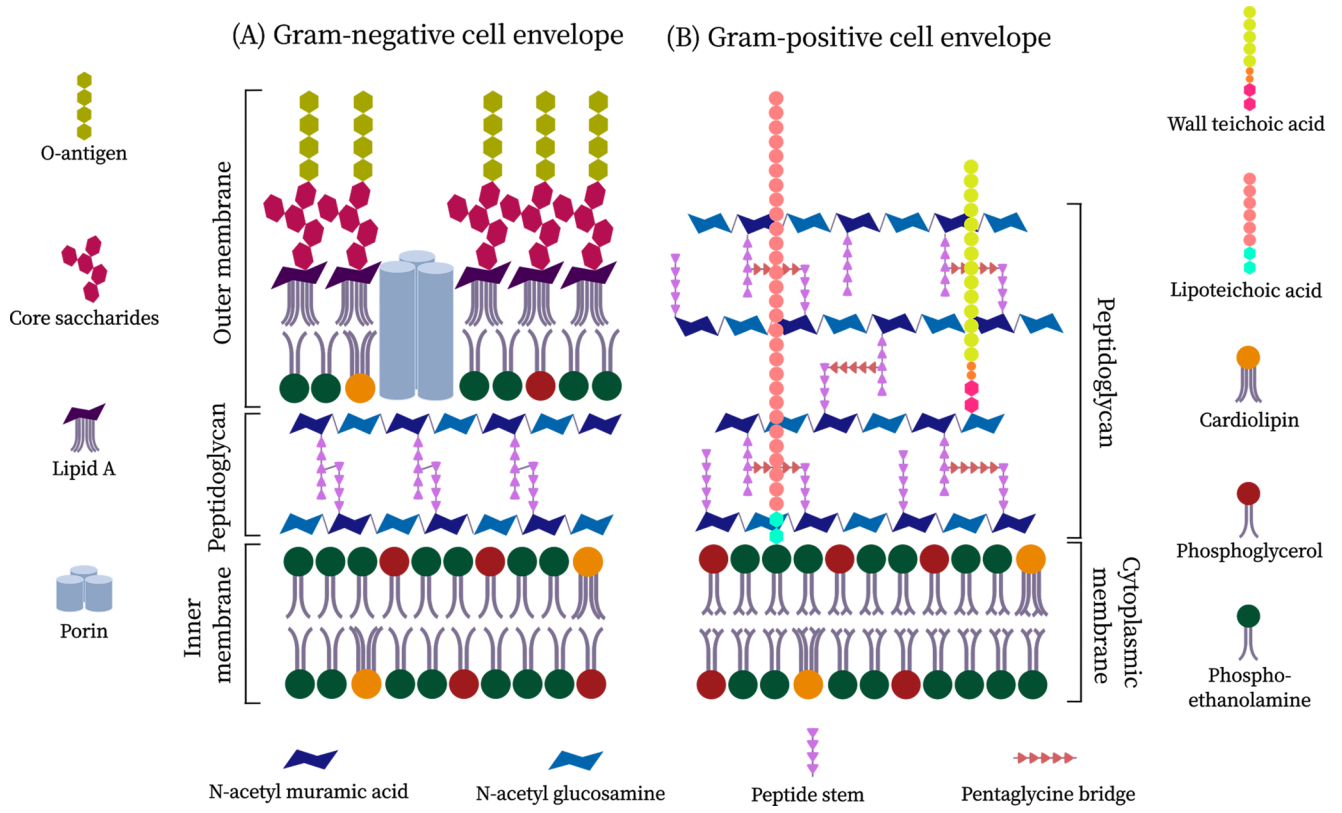

Figure 1. Schematic illustration of the bacterial cell envelope components for (A) Gram-negative (*E. coli*) and (B) Gram-positive (*S. aureus*) bacteria, representing the differences in their structures.

Despite efforts toward the progress of these experimental techniques and given the underlying complexity of the envelope, it is challenging to decipher detailed molecular-level interactions with different parts of the bacterial cell envelope. Molecular dynamics (MD) simulations have evolved as a powerful nanoscopic tool to understand the structural, mechanical, dynamic, and barrier properties of the cellular membrane.[3] Studies on model development of the bacterial cell envelope and their utility to understand interactions with various proteins, peptides, surfactants, and small molecules are necessary to develop better strategies to fight bacterial infections. These studies will help gain insight into the biologically relevant processes that involve specific interactions with bacterial cell envelopes and also aid in the development of novel antimicrobial products.

In this review, we provide a perspective on the development of molecular models and MD simulation techniques that have been used to understand the structural properties of various components of the bacterial cell envelope. The review begins with a detailed structural description of the cell envelopes of Gram-negative and Gram-positive strains. Next, we review the MD literature in three broad sections that cover structural aspects and the models developed to study the outer membrane of Gram-negative bacteria, the peptidoglycan or cell walls, and the inner phospholipid bilayer membranes of both Gram-positive and negative strains. Following this, we turn our attention to the translocation of molecules through different sections of the bacterial cell envelope, which includes transport through outer membrane porins and peptidoglycan. Since surfactants are widely used as antimicrobials, we have a section on studies concerned with the interactions of surfactants with the inner membrane and peptidoglycan. The last section is concerned with simulations of antimicrobial peptides with different parts of the cell envelope, and the review ends with a conclusion and perspective section.

STRUCTURE OF THE BACTERIAL CELL ENVELOPE

In contrast to the mammalian plasma membrane, which consists of a phospholipid membrane, the bacterial cell envelope has a complex architecture bearing topologically distinct membranes arranged in a tiered manner.[10] Additionally, the structures of Gram-positive and Gram-negative bacteria cell envelopes have distinct differences (Figure 1). The presence of lipopolysaccharide (LPS) molecules, made up of lipids and sugars, in the outer membrane of Gram-negative strains serves as the primary external barrier. The main external barrier in the case of Gram-positive bacteria is a thicker peptidoglycan layer without the presence of the outer LPS membrane. The peptidoglycan layer, also known as murein, is a mesh-like structure that is considered to be the largest macromolecule with strands of disaccharides interconnected with peptides.[11] Peptidoglycan provides structural rigidity and shape to the cell and is also referred to as the cell wall. In the case of Gram-negative strains, a thinner peptidoglycan layer is sandwiched between the outer LPS membrane and the inner phospholipid bilayer to form the intervening region known as the periplasm. The periplasm contains enzymes, anchoring proteins and metabolites that facilitate protein folding and sensing.[12] The cytoplasmic phospholipid membrane and peptidoglycan layers are present in both Gram-negative and Gram-positive strains with specific compositional differences.

Gram-Negative Bacterial Cell Envelope. The trilayer assembly[10] (Figure 1) of the cell envelope, namely the inner membrane, peptidoglycan, and outer membrane, makes Gram-

https://doi.org/10.1021/acs.langmuir.3c03474
Langmuir 2024, 40, 7791−7811

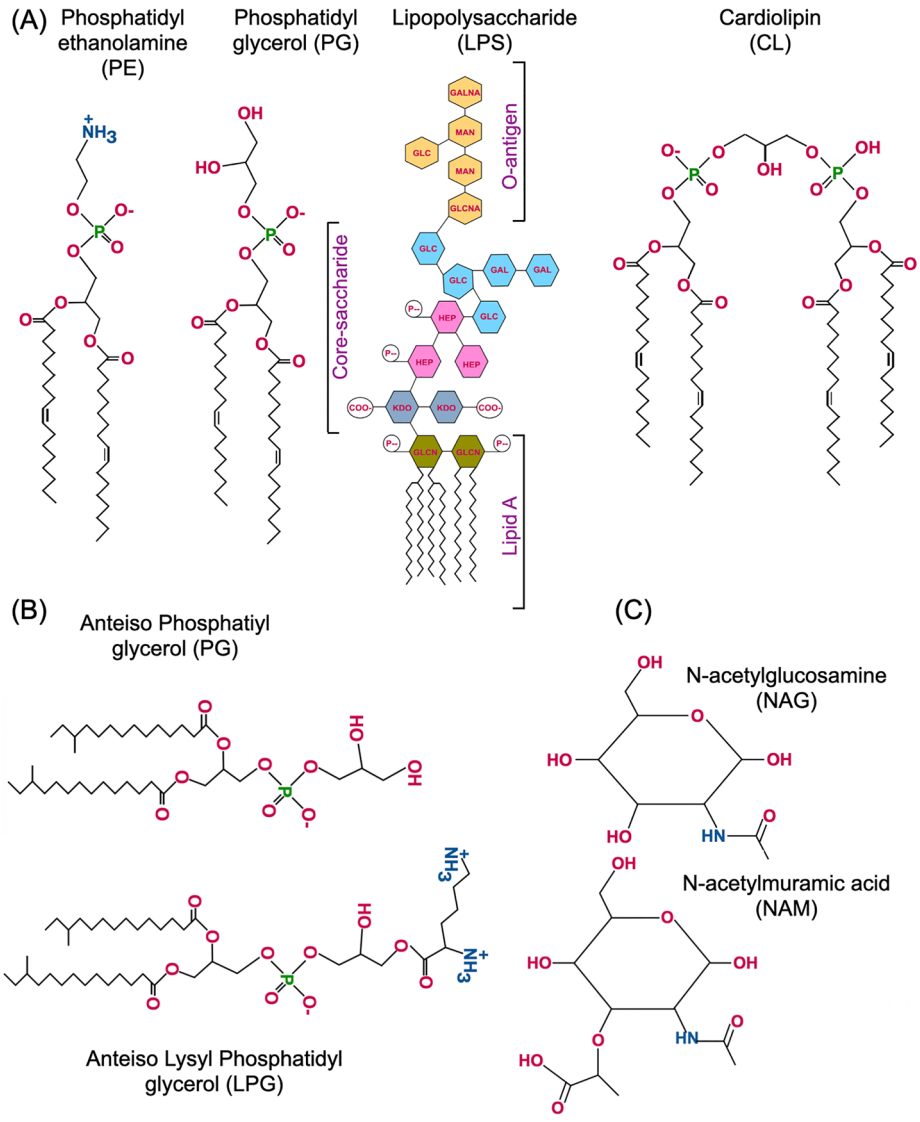

Figure 2. (A) Lipids present in inner and outer membranes of Gram-negative bacteria (*E. coli*). (B) Anteiso lipids present in cytoplasmic membrane of Gram-positive bacteria (*S. aureus*). (C) Glycan residues *N*-acetylglucosamine and *N*-acetylmuramic acid are the molecular building blocks of peptidoglycan.

negative bacteria resilient toward antimicrobials, providing a protective barrier against hostile environments.[13] We will use *Escherichia coli* (*E. coli*), an archetypical bacterium, as a representative of Gram-negative bacteria.

Outer Membrane. The outer membrane is an asymmetric bilayer with a lower leaflet composed of phospholipids such as phosphatidylethanolamine (PE), phosphatidylglycerol (PG), and cardiolipin (CL) and an upper leaflet composed of LPS molecules. Bacteria have evolved to allow the selective passage of the molecules through the outer membrane, which serves as a barrier for harmful molecules and allows selective transport of ions and nutrients essential for the bacteria.

The lipid composition in lower leaflet of the outer membrane (Figure 1A) varies between bacterial strains. For instance, *E. coli* has a PE:PG:CL molar ratio of 90:5:5, while *Pseudomonas aeruginosa* has a 60:27:13 composition.[14,15] The PE lipids are zwitterionic, PG and CL are anionic, and CL is four-tailed lipid molecule (Figure 2).[16] The LPS molecules in upper leaflet of the outer membrane are amphipathic in nature[17] (Figure 2). Bacteria show a diverse variation in the structure of LPS molecules based on species, strain, and the life cycle. The LPS molecules are akin to polymeric brushes anchored on the bilayer by phylogenetically conserved lipid A.

Lipid A is composed of diglucosamine diphosphate with four to six lipid chains, forming the hydrophobic anchor for LPS in the bilayer (Figure 2A). Toward the extracellular side, lipid A is connected to core saccharides, which are in turn connected to O-antigen. The sugars in the core saccharides are further classified as inner and outer core sugars, which are commonly referred to as Re-LPS and Ra-LPS, respectively. The sugars that make up the inner and outer core vary across bacterial strains. For example, the inner core for *E. coli* consists of 2-keto-3-deoxyoctulosonate (KDO) and L-glycero-D-manno-heptose (HEP) sugars, and the outer core in addition contains D-glucose (GLC) and D-galactose (GAL) sugars (Figure 2A). An LPS molecule with O-antigen units is termed as smooth LPS, while an LPS molecule in the absence of O-antigen is referred to as rough LPS. The O-antigen saccharides are polymers of various lengths of repeating sugar units (up to ~100). A few Gram-negative bacteria also contain glycolipids,

https://doi.org/10.1021/acs.langmuir.3c03474
Langmuir 2024, 40, 7791−7811

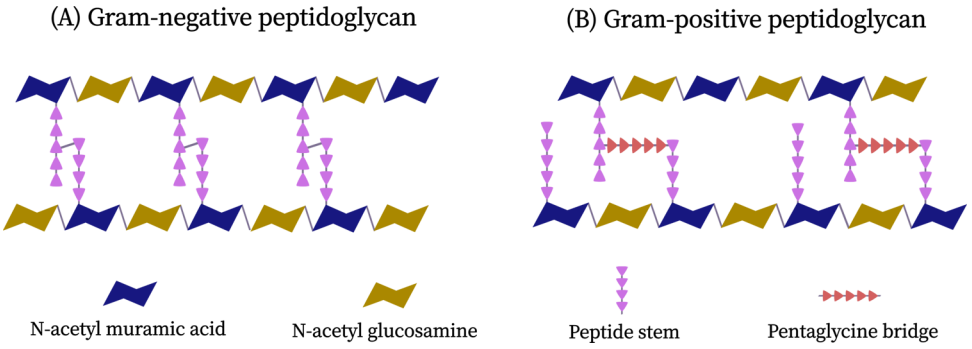

Figure 3. Schematic representation of peptidoglycan structure for typical (A) Gram-negative (*E. coli*) and (B) Gram-positive (*S. aureus*) bacteria, indicating the differences in peptide stems and cross-linking.

such as enterobacterial common antigens[18] and capsular polysaccharides,[19] along with LPS.

Peptidoglycan. Peptidoglycan is a mesh-like structure composed of polymeric glycan strands cross-linked by peptide stems (Figure 3).[11] Glycan strands are made up of disaccharides of *N*-acetylglucosamine (NAG) and *N*-acetylmuramic acid (NAM). These strands are interconnected through penta-peptides covalently bonded with a lactyl moiety of each NAM residue. The residue sequence of these peptide stems is L-alanine (L-Ala), D-*iso*-glutamate (Glu), *meso*-diaminopimelic acid (m-A_2pm), and D-alanine (D-Ala) (Figure 3). The peptide stems in peptidoglycan have dual functions: to connect the glycan strands through cross-linking and to serve as an anchor to covalently hold membrane-bound proteins.[20,21] The cross-linking between peptides of adjacent strands occurs by bridging a covalent bond between the m-A_2pm of the acceptor peptide and the penultimate D-Ala of the donor peptide (Figure 3). During this bridging, the terminal D-Ala in the donor peptide is eliminated.

In its simpler architecture, peptidoglycan in Gram-negative species consists of a monolayer,[22] bearing relatively longer strands of glycans, while peptidoglycan in Gram-positive strains is relatively thicker with shorter glycan strands.[23,24] A cryo-transmission electron microscopy study[25] revealed thicknesses of 6.3 nm in *E. coli* and 2.4 nm in *P. aeruginosa*, consistent with other atomic force microscopy and electron microscopy studies.[26] The extent of peptide cross-linking is correlated with the peptidoglycan thickness. In *E. coli* strains, 40−60% of the muropeptides are cross-linked. The spacing between glycan strands is around 1.25 nm with the disaccharide (NAG-NAM) units having a length of 1.03 nm. The surface area per disaccharide varies between 1.3 and 2.5 nm^2.[27−29] The average length of glycan chains and their distributions depend on the species and growth conditions.[30] For Gram-negative species, the average chain length is in the range of 20−40 disaccharide units.[30,31] In *Helicobacter pylori*, the chains are much shorter with average lengths of less than 10 disaccharide units.[32]

Two contrasting models have been proposed for the orientation of glycans with reference to the cytoplasmic membrane. In the classic "layered" model, the glycan chains are parallel to the cytoplasmic membrane, running as hoops or helices along the short axis of the cell sacculus.[22,33] In the scaffold model, glycan chains run in a direction perpendicular to the cytoplasmic membrane.

Cytoplasmic Inner Membrane. Like the lower leaflet of the outer membrane, the inner membrane of Gram-negative bacteria is composed of PE, PG, and CL, with compositions varying across the strains. A typical composition has a molar ratio of 75:20:5 (PE:PG:CL). Being the major component of the inner membrane, PE has been extensively used in inner membrane models. Although present in lower concentrations, the importance of the anionic PG and CL lipids has been implicated in various phenomena. PG lipids are known to provide stability to bacterial membranes by enhancing interlipid interactions.[34] Though smallest in composition, CL is also found to play a significant role. It has been observed that the osmosensory transporter ProP at the bacterial poles increases with the CL content and, hence, regulates the osmotic response of bacteria.[35] CL is also crucial in the formation of nonlamellar intracellular membranes in the cytoplasm[36] and has recently been shown to modulate peptide interactions.[37] It is a vital component of the membrane in the polar and septal regions of the bacteria.[38] Lipid tails are also known to possess specific variations in tail structure. Using mass spectroscopy methods, it has been shown that bacterial lipid tails can have cyclic moieties,[39,40] which influence the structural properties of the membrane. The importance of the cyclopropane moiety present in lipid tails of some Gram-negative bacteria has been investigated using nuclear magnetic resonance (NMR).[41] Simulation studies of the inner membrane of *E. coli* composed of PE and PG lipid tails containing cyclopropane have been carried out at compositions that reflect the life cycle of the bacteria, namely early log, mid log, stationary, and the dead stage.[42,43] These studies showed the influence of the diversity of lipid compositions and asymmetry on the structure and dynamics of the inner membrane. Cyclopropane present in fatty acid chains induces local disordering and reduced chain packing, resulting in a higher surface area per lipid. These studies highlight the need for developing more realistic and complex inner membrane models.

Gram-Positive Bacterial Cell Envelope. The outer LPS membrane present in Gram-negative strains is replaced by a thicker peptidoglycan layer (Figure 1) in Gram-positive bacteria, which helps bacteria to survive in harsh environments and withstand the turgor pressure exerted on the inner membrane.[44] Another contrasting feature of the Gram-positive cell envelope is the presence of teichoic acids.[45] These long anionic polymers composed of glycerol phosphate, glucosyl phosphate, or ribitol phosphate are threaded across the peptidoglycan layer. The wall teichoic and lipoteichoic acids are anchored onto the peptidoglycan layer and membrane lipids, respectively (Figure 1B). *Staphylococcus aureus* (*S. aureus*) will be used as a representative for Gram-positive bacteria in the text.

https://doi.org/10.1021/acs.langmuir.3c03474
Langmuir 2024, 40, 7791−7811

Peptidoglycan. The basic network structure of the peptidoglycan layers is similar in both Gram-negative and Gram-positive bacteria, having glycan strands made up of disaccharides of NAG and NAM units cross-linked by peptides (Figures 1 and 3). In Gram-positive bacteria, the peptidoglycan layer is much thicker (20−80 nm), with many layers stacked and connected covalently to each other, unlike the monolayer structure found in Gram-negative *E. coli*. The thickness of peptidoglycan measured in cryo-electron microscopy (cryo-EM) studies was 19 nm for *S. aureus* and 33 nm for *Bacillus subtilis*.[23,24] The strains of *S. aureus* have a relatively higher percentage of cross-linking in the range of 74−92% due to the multilayered stacking of peptidoglycan, enabling cross-linking in two orthogonal directions.[46,47] In *S. aureus*, the average length for glycan chains is 6 disaccharide units,[48] while in contrast, the average chain length in other Gram-positive species can be significantly longer, ranging between 50 and 250 disaccharide units.[49−51] Peptidoglycan in Gram-positive strains has distinct chemical differences when compared to that in Gram-negative strains. In particular, the amino acids in Gram-positive bacteria (*S. aureus*) are D-*iso*-glutamine (Gln) and L-lysine (Lys), in contrast to D-*iso*-glutamate (Glu) and *meso*-diaminopimelic acid (m-A_2pm) that are present in Gram-negative peptidoglycan in *E. coli*. Another key difference is the peptide cross-linking (Figure 3). In Gram-positive bacteria, the peptide stems are interconnected via a pentaglycine branch, extending from the Lys in one peptide stem to the penultimate D-Ala in a neighboring stem peptide. Similar to the Gram-negative peptidoglycan layer, the terminal D-Ala of the donor peptide is eliminated due to peptide cross-linking.

Cytoplasmic Inner Membrane. The cytoplasmic membrane in Gram-positive bacteria contains lipid tails with branched groups, and the headgroups of such lipids are also modified to include amino acid residues, such as alanine and lysine, to gain resistance against cationic antimicrobials.[52−54] The modified lipids are Ala-PG and Lys-PG (Figure 2).

While the phospholipids in the inner membrane of Gram-negative bacteria typically bear both saturated (C16:0) and unsaturated (C16:1, C18:1) carbon chains, in Gram-positive bacteria, branched fatty acids (Figure 2) with a significant distribution of "anteiso" C15:0 and C17:0 chains are present.[55,56] If a methyl branch occurs at the penultimate carbon atom, these chains are referred to as "iso" chains. The fatty acid composition, especially the inclusion of branched lipids, is expected to enhance membrane fluidity, interdigitation, and chain disordering.[57] Although the lipid compositions vary with growth conditions, experimental studies with the cells harvested at pH = 6.5 have reported 57% PG, 38% Lys-PG, and 5% CL in the cytoplasmic membrane of *S. aureus*.[55,58]

MD SIMULATIONS OF THE BACTERIAL CELL ENVELOPE

Molecular dynamics simulations have been extensively utilized to study biological membranes. Depending on the level of description of interactions between atoms and coarse-grained moieties, the molecular force fields in simulations consist of either all-atom, united-atom, or coarse-grained bead interactions, and the bacterial cell envelope has been modeled using all three frameworks. The detailed all-atom force fields account for the degree of freedom of all atoms in the system (including hydrogen atoms), making this approach computationally intensive. CHARMM,[80] AMBER,[81] and Slipids[82] are widely used all-atom force fields. The length and time scales typically accessible with all-atom simulations limit studies of biological phenomena, which require longer times or involve systems with several million atoms. To overcome these limitations, united-atom and other coarse-grained models have evolved as faster and reasonably accurate alternatives to the all-atom molecular models. The philosophy of united-atom force fields, such as GROMOS,[83] relies on grouping the hydrogen atoms with the aliphatic carbons to create a "united-atom", which is subsequently parametrized. At a higher level of coarse-graining, several atoms are grouped to form a larger-sized entity, referred to as a bead. In coarse-grained models such as Martini,[84] the interactions between beads are parametrized to capture the essential chemistry of the constituent building atoms.[85] This coarsening overcomes the computational effort needed to investigate molecular systems and profoundly advances the feasibility of attaining temporal and spatial evolution of mesoscale systems. The advantage of reduced computational overhead and the ability to sample greater length and time scales come at the loss of molecular details.[86] Hence, extensive testing of coarse-grained force fields such as Martini is needed. Since the outer membrane and the peptidoglycan layers of the bacterial cell envelope are composed of sugars, the accuracy of the recent Martini models for these components of the bacterial cell envelope needs to be tested against accurate all-atom force fields.[79,87−89] In what follows, we summarize the literature concerning MD simulations of different components of the bacterial cell envelope using all-atom, united-atom, and coarse-grained descriptions.

Simulations of the Gram-Negative Outer Membrane. Molecular modeling of the bacterial cell envelope of Gram-negative bacteria (Figure 1) has evolved from early studies of smooth LPS monolayers[59] to comprehensive models of the cell envelope[76] comprising the outer membrane, peptidoglycan, inner membrane, and proteins. Over the last two decades, most outer membrane models have been dedicated to *E. coli* and *P. aeruginosa*, and the corresponding simulation literature is listed in Table 1. Recently, outer membrane models for other bacteria such as *Moraxella catarrhalis* have also been developed.[78] Few studies have been conducted in the past to highlight the need for distinct models and to bring out the influence of species-dependent lipid chain length on membrane properties such as the lateral area, thickness, diffusivity, and other mechanical properties.[67,71] The inclusion of the LPS modeler on the CHARMM-GUI web server[73] has revolutionized the construction of outer membrane models for bacteria. The web server hosts a rich database of LPS molecules for different bacterial species, enabling MD studies of the bacterial membrane with species-specific lipid architecture.

Kotra et al.[59] developed one of the earliest smooth LPS atomistic outer membrane monolayer models to represent the outer leaflet of the outer membrane. This study on the *E. coli* membrane demonstrated the role of divalent ions in stabilizing the LPS assembly, which was previously observed in experiments.[90] Lins and Straatsma[60] developed an all-atom asymmetric outer membrane model for *P. aeruginosa* comprising rough LPS molecules and phospholipids (PE) to obtain a transmembrane electrostatic potential of about −100 mV, which was in good agreement with that of −85 mV reported experimentally.[91] Using a similar model,[61] the area per LPS of 1.06 nm^2 was found to be in good agreement with the experimental value of 1.08 nm^2, and the dynamics for the

https://doi.org/10.1021/acs.langmuir.3c03474
Langmuir 2024, 40, 7791−7811

Table 1. Summary of the Literature of Lipopolysaccharide and Outer Membrane Simulations[a]

year	species	force field	lipid model
1999[59]	*E. coli*^{M}	GLYCAM	smooth LPS
2001[60]	*P. aeruginosa*^{A}	GLYCAM93, AMBER95	rough LPS, PE
2007[61]	*P. aeruginosa*^{A}	GLYCAM93, AMBER96	rough LPS, PE
2011[62]	*E. coli*^{A}	GROMOS53A6	rough LPS, PE, PG, CL
2012[63]	*P. aeruginosa*^{A}	GLYCAM06	rough LPS, PE
2013[64]	*E. coli*^{S}	CHARMM36	lipid A, rough and smooth LPS
2015[66]	*E. coli*^{A}, *P. aeruginosa*^{A}	Martini	rough and smooth LPS, PE
2016[65]	*P. aeruginosa*^{A}	Martini	rough LPS, PE
2016[67]	various bacteria^{S}	CHARMM36	lipid A
2016[68]	*E. coli*^{A}	Martini	Re-LPS, Ra-LPS, PE
2017[69]	*E. coli*^{A}	Martini	Re-LPS, PE, PG, CL
2017[70]	*E. coli*^{A} and *P. aeruginosa*^{A}	CHARMM	rough and smooth LPS, PE, PG, CL
2017[71]	various bacteria^{A}	Martini	lipid A, PE
2018[15]	*P. aeruginosa*^{A}	GLYCAM06, Slipids	lipid A, PE, PG, CL
2018[72]	*S. enterica*^{S}	CHARMM36	lipid A, Rc LPS
2019[73]	Membrane Builder	CHARMM36	LPS
2019[74]	*E. coli*^{A}	Martini	smooth LPS, PE, PG
2019[75]	*E. coli*^{A}	CHARMM36	rough LPS, PE, PG, CL
2019[76]	*E. coli*^{A}	CHARMM36	Ra-LPS, PE, PG, CL
2019[77]	*E. coli*^{A}	Martini	rough and smooth LPS, PE, PG, CL
2020[78]	*Moraxella catarrhalis*^{S}	CHARMM36	LOS
2024[79]	*E. coli*^{A}	Martini 3	smooth LPS

[a]PE, phosphatidylethanolamine; PG, phosphatidylglycerol; CL, cardiolipin; and LOS, lipooligosaccharide. ^{M}Monolayer. ^{A}Asymmetric bilayer. ^{S}Symmetric bilayer.

O-antigen units were faster when compared with the core sugars.

In an electroporation study, Piggot et al.[62] used united-atom models of the *E. coli* outer membrane and the cytoplasmic membrane of *S. aureus* to show that poration occurred at lower voltages for the *S. aureus* membrane. The differences were attributed to the lower mobility of LPS molecules compared to that of phospholipids. The GLYCAM06 force field for *P. aeruginosa* developed by Kirschner et al.[63] reproduced the experimental area per LPS quite accurately and found the orientational behavior of LPS molecules to conform to data from Fourier transform infrared spectroscopy.[92] The model also captured the enhanced permeability of water in the liquid crystalline phase, which was previously observed using neutron scattering.[93] Wu et al.[64] performed a combined MD simulations and experimental study, where they developed an all-atom symmetric outer membrane model for *E. coli* in the CHARMM36 force field. Interproton distances from the simulations agreed well with those derived from NMR experiments for the O-antigen units. The variations in the structure and dynamics of the membrane were studied as a function of different lengths of LPS molecules.

Compared to atomistic models, coarse-grained models are ideal alternatives to study the complex outer membrane of bacteria,[84] and several Martini models describing the outer membrane have been developed over the past decade. Van Oosten and Harroun[65] developed a Martini membrane of *P. aeruginosa* with upper and lower leaflets composed of rough LPS and PE lipids, respectively. They used both the standard[84] and polarizable Martini water models[94] and compared the area per lipid and the membrane thickness with all-atom simulations. Interestingly, the structural properties of the outer membrane were accurately reproduced using the standard Martini water model. Ma et al.[66] used a more detailed Martini model of the outer membrane with smooth LPS and found the gel to liquid-crystalline phase transition temperature at 314 K, which was in good agreement with the experimental value of 310 K for *E. coli*.[95,96] Increasing the concentration of PE lipids in the upper leaflet resulted in higher melting temperatures, lowered the area per lipid, and increased chain order. These Martini models were further refined with small modifications in a study by Hsu et al.[68] The improved model was parametrized using the simulation data on a united-atom model of the outer membrane. This outer membrane model was then utilized to study the interactions with pristine fullerenes. The membrane model was further expanded by Shearer et al.[77] by including O-antigen units.

To understand the effect of diversity in lipid A molecules, Ma et al.[71] constructed Martini models for seven different bacterial species to infer that the structural properties and the

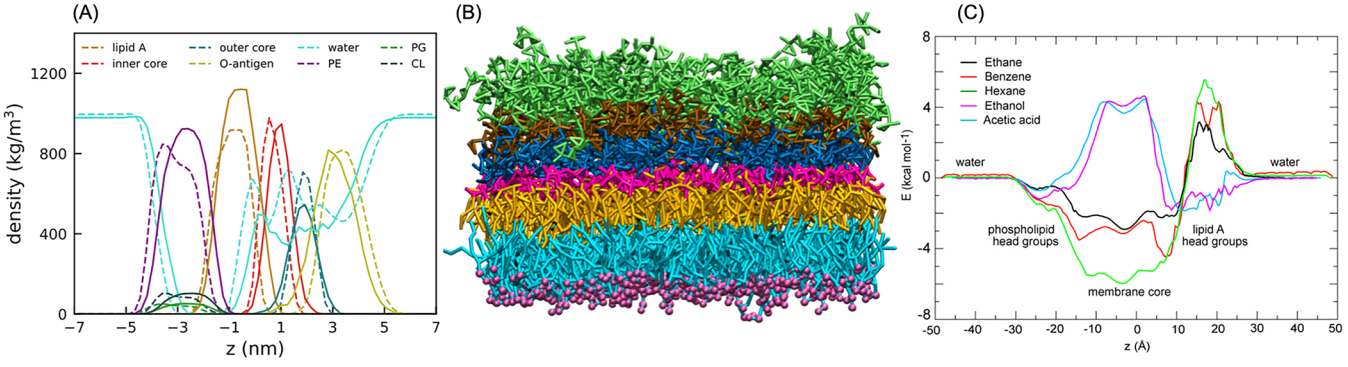

Figure 4. (A) Comparison between all-atom and coarse-grained models of outer membranes, showing the mass density profiles for phospholipids (PE, PG, CL) and various regions of LPS, namely lipid A, inner and outer cores, and O-antigen. (B) The coarse-grained model of the outer membrane of *E. coli*, recently developed in the Martini 3 framework. (C) Interaction energies for insertion of small molecules into Re-LPS. Panels (A) and (B) are adapted with permission from ref 79. Copyright 2023 American Chemical Society. Panel (C) is reproduced with permission from ref 99. Copyright 2016 American Chemical Society.

https://doi.org/10.1021/acs.langmuir.3c03474
Langmuir 2024, 40, 7791−7811

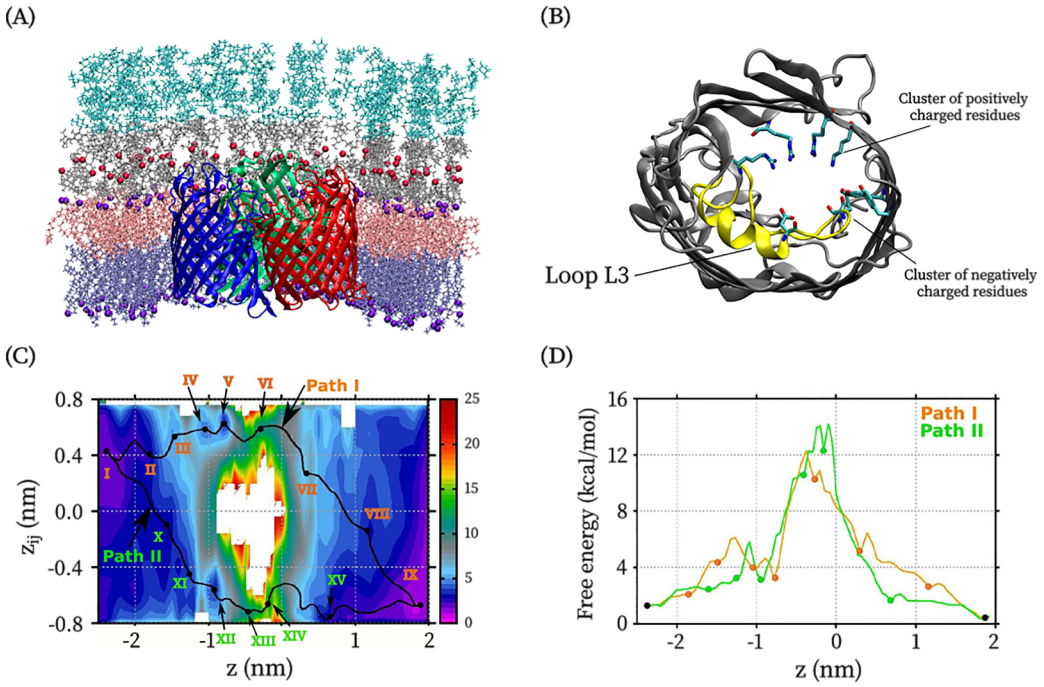

Figure 5. (A) Illustration of the trimeric β-barrel porin OmpF (PDB ID: 3POX) in the outer membrane of *E. coli.* (B) View of the constriction region of OmpF formed by the loop L3 and lined by oppositely charged residues (PDB ID: 2OMF). (C) 2D free energy landscape for the permeation of the antibiotic ciprofloxacin through OmpF. The string method was used to calculate two minimum free energy paths, represented by black lines. z_{ij} is an orientation vector along ciprofloxacin, and z is the distance along the OmpF channel. (D) The free energy profile along the two identified minimum free energy paths in (C), where the points correspond to the Roman numerals in (C). Panels (C) and (D) are reproduced with permission from ref 139. Copyright 2021 American Chemical Society.

phase transition temperatures vary across bacterial strains with a strong influence of the chain and headgroup characteristics of lipid A on membrane properties. Martini simulations have also been employed for bacterial membranes in conjunction with outer membrane porins (OmpA, OmpX, BtuB, FhuA, OmpF, EstA).[77] The study concluded that the protein−membrane interactions are dependent on the description of LPS molecules (rough LPS versus smooth LPS), highlighting the significance of including O-antigen units in LPS models. An interesting finding in this study was the scarcity of cardiolipin molecules in the neighborhood of the proteins. O-antigen is known to impart additional mechanical strength to the outer membrane.[74]

While the Martini force field has been widely used to study lipids, the interactions of sugar molecules were not accurately captured in earlier versions of the force field.[97,98] Using the recently developed Martini 3 force field, which overcomes the shortcoming of the sugar parametrization, Vaiwala and Ayappa[79] developed coarse-grained models of the outer membrane of *E. coli* (Figure 4A,B). The parametrization was systematically evaluated for symmetric bilayers of lipid A and rough LPS as well as the asymmetric outer membrane composed of smooth LPS and phospholipids. The model membranes were found to accurately reproduce the solvent accessible surface area, membrane thickness, and area per lipid when compared with the all-atom models in the CHARMM36 force field. Significantly, calcium binding with phosphate and carboxylate groups of LPS was also captured. The data on mean square displacements over 8 μs simulations revealed the enhanced diffusivity of the inner leaflet lipids when compared with the sluggish LPS molecules.

Bacterial membranes undergo structural and chemical modifications in order to reduce their susceptibility to antibiotics, giving rise to resistant strains. MD simulations have the capacity to incorporate the effect of modifications in the membrane on their properties to explain, at the molecular level, how resistant bacterial strains are advantageous relative to the wild type. In one such study, Rice and Wereszczynski[72] performed all-atom simulations of the LPS membrane of *Salmonella enterica* serovar Typhimurium, incorporating the structural modifications, which are known to enhance virulence and survival under conditions of stress.[100] Among the different modifications, the presence of a positively charged amino-arabinose sugar attached to the phosphate headgroup reduced the divalent cation density, rendering the LPS less susceptible to antimicrobials. In a related MD simulation by Luna et al.,[101] the structural variations in the lipid A of *Vibrio cholerae* differentiated by amino functional groups and additional acyl chains were studied to gain insights into resistant strains. The resulting increase in bilayer stability upon the addition of cationic functional groups in LPS was related to the increased resistance to polymyxin antibiotics.

Proteins are an integral component of the outer membrane, constituting around 25−30% of the membrane surface area, and they functionally play the role of transporters and channels for small molecules across the membrane.[102] Recent bacterial imaging studies using atomic force microscopy have reported the abundance of trimeric porins in the outer membrane of *E. coli*.[103] Hence, the physical properties of the membrane, such as its curvature, fluidity and permeability, are likely to be influenced by the presence of proteins, which are embedded with β-barrels in the lipid environment of the outer membrane (Figure 5A). Thus, outer membrane models are incomplete

https://doi.org/10.1021/acs.langmuir.3c03474
Langmuir 2024, 40, 7791−7811

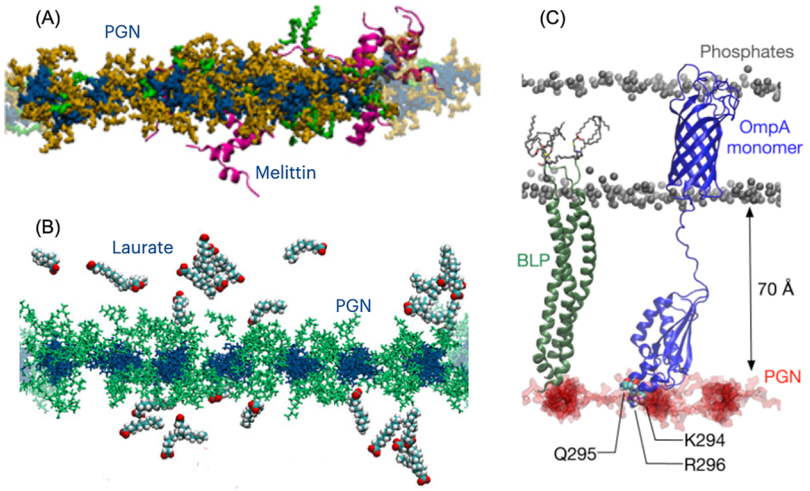

Figure 6. (A) Melittin peptide has a strong affinity to bind with the peptidoglycan network. Reproduced with permission from ref 122. Copyright 2022 American Vacuum Society. (B) Single surfactant molecules translocate through peptidoglycan, but an aggregate is prevented from crossing the barrier. Reproduced with permission from ref 112. Copyright 2022 American Chemical Society. (C) Outer membrane porin OmpA interacts with peptidoglycan (PGN), and Braun's lipoprotein (BLP) lowers the distance between peptidoglycan and the outer membrane. Reproduced with permission from ref 120. Copyright 2017 Biophysical Society.

without the incorporation of proteins. Hsu et al.[69] built a coarse-grained Martini construct of the *E. coli* inner and outer membranes together with the multidrug efflux pump AcrBZ-TolC and a varying number of proteins to simulate the effect of protein crowding on the properties of the membrane. The study reported variations in the membrane curvature depending on the size and type of transmembrane proteins. The analysis of mean squared displacement and lipid fluidity revealed a slower and strongly correlated motion of LPS in the outer membrane compared to the more fluid-like motion of the phospholipids. Enhanced interactions with cardiolipin molecules led to their enrichment around specific proteins. Using all-atom simulations, Lee et al.[70] reported the thinning of the outer membrane of *P. aeruginosa* surrounding the protein OprH. The readjustment of acyl chains improved the hydrophobic matching with the protein residues and provided enhanced stability to the membrane. Goose and Sansom[104] simulated coarse-grained models of multiple outer membrane proteins (FhuA, LamB, NanC, OmpA, and OmpF) embedded in a phospholipid bilayer and reported reduced diffusivity of lipids surrounding these proteins.

The LPS leaflet has been observed to exhibit subdiffusive properties in all-atom simulations spanning a few microseconds,[72] owing to the bulkiness and strong electrostatic interlinking of the lipids. This electrostatic network formed by divalent cations stabilizes LPS−protein interactions, as observed in the crystal structure of OmpE36 porin of *Enterobacter cloacae*.[105] By computing the charge distribution of divalent ions around OmpE36, the subsequent all-atom simulation study by Kesireddy et al.[75] confirmed the role of divalent cations in stabilizing the interactions between the negatively charged phosphate headgroups in the lipid A of LPS and various negatively charged residues of the porin in the vicinity of these headgroups.

Peptidoglycan Models and Structure. There are only few simulations studies that model the peptidoglycan layer (Figure 3). The scope of developing a coarse-grained Martini model of the peptidoglycan layer has been challenging due to the shortcomings in Martini models of sugars and amino acids,[86,113] which have been overcome in the recent Martini 3 version of the force field. According to initial studies on Gram-negative *E. coli* strains using computer simulations, it was hypothesized that the glycan chains orient in either regular or irregular patterns parallel to the plasma membrane and that the peptidoglycan structure is porous for the transport of nutrients and other small molecules.[114,115] This layered model for the tertiary structure of Gram-negative peptidoglycan was then superseded with the scaffold model, in which the glycan strands are oriented perpendicular to the plasma membrane and the peptide bridges run parallel to the membrane, accommodating the experimental data on glycan chain length distributions and cross-linking.[116]

A murein fragment composed of disaccharides and muropeptides L-Ala−D-*iso*-Gln−L-Lys−$(Gly)_5$−D-Ala−D-Ala was relaxed in a simulation study using a molecular mechanics force field.[117] A refined scaffold model for Gram-positive *S. aureus* was proposed. Accordingly, both glycan strands and muropeptides orient in a direction orthogonal to the plasma membrane, and the peptides adopt zigzag conformations along the glycan strands. In agreement with experimental evidence, the murein martrix resulted in a high degree of cross-linking (83%). In a more extensive study,[11] an atomistic model for Gram-negative *E. coli* was developed using the CHARMM force field and simulated to bring out the configurational features of the glycans and peptides at the molecular level. The peptides were configured along the glycan strands with 4-fold symmetry of native orientation. The murein thickness and the pores in the murein matrix were found to be consistent with experimental data, and the tensile elasticity was anisotropic due to glycans and peptides orienting in two orthogonal directions. A murein model for *B. subtilis* was simulated using all-atom simulations, and the study revealed a circumferential orientation of glycan strands in the rod-shaped Gram-positive sacculus, which is consistent with electron cryo-tomography data.[44]

GROMOS compatible force field parameters were developed for peptidoglycan in a study on an outer membrane protein (OmpA) binding to peptidoglycan.[118] This study revealed that the peptidoglycan binding to outer membrane proteins from different strains of *E. coli* is conserved, although

https://doi.org/10.1021/acs.langmuir.3c03474
Langmuir 2024, 40, 7791−7811

the binding strength is likely to vary across the outer membrane proteins and strains studied. The noncovalent and flexible anchoring of outer membrane proteins to peptidoglycan provides mechanical stability to the cell wall.[119] A role of Braun's lipoprotein in mediating the peptidoglycan binding to outer membrane proteins has also been investigated using all-atom MD simulations[120] (Figure 6C). The conformational changes associated with tilting and bending in Braun's lipoprotein bring the cell wall closer to the binding domains of the outer membrane proteins, and only the dimeric state of OmpA was found to attach to the peptidoglycan in the absence of the lipoprotein. These studies provided, for the first time, molecular insights into the protein-mediated coupling that exists between the outer membrane and peptidoglycan, an essential ingredient in understanding the complex role played by the periplasm.

Resistant strains of bacteria have a chemically modified structure of peptidoglycan. For example, the muramic acid residues in lysozyme-resistant *S. aureus* are O-acetylated at O6 oxygen. This modification results in structurally unstable conformations of peptide stems in the vicinity of lysozyme, which in turn causes steric hindrances at the active site of lysozyme, preventing cleavage of glycosidic linkages.[121]

Recently, more realistic models for *E. coli* and *S. aureus* peptidoglycan cell walls have been developed at atomistic and coarse-grained scales, and their interactions with small actives have been examined.[112,113,122] The contrasting features between peptidoglycan of Gram-negative and Gram-positive strains emerged from a simulation study using monolayered constructs of peptidoglycan.[122] The area per disaccharide, charge density, electrostatic potential, and pore size were found to be lower in magnitude for the model *S. aureus* cell wall when compared with those of the *E. coli* model. In particular, a higher charge density and greater hydration were observed for the Gram-negative peptidoglycan. These structural differences are likely to impact the interactions of cell walls with antimicrobial peptides and small molecules.

Simulations of Cytoplasmic Inner Membranes. The literature concerned with simulations of the inner membrane of both Gram-negative and Gram-positive strains are summarized in Table 2. Molecular models of the inner membrane of Gram-negative bacteria have also emerged from PE bilayer models to a more accurate and detailed model having multicomponent lipid compositions,[106] including lipids having cyclic moieties, which were shown to effect the structural properties of the membrane. Although present in low concentrations (~5%), the inclusion of cardiolipin in membrane models has gained importance.[4,62] Cardiolipin binds to particular transporter proteins.[108] In a study using all-atom force fields,[56] 19 different types of phospholipids were assembled to construct a complex cytoplasmic membrane of *S. aureus*. The lipid headgroups were representative PG, Lys-PG, and cardiolipin molecules, while the lipid tails carried saturated carbon branches of "iso" and "anteiso" types (Figure 2). Different C−H ordering, chain interdigitation, and water permeation in the multicomponent membrane revealed diverse membrane properties.

In another study on *S. aureus*, the conformational dynamics of lipid II in the model membrane have been investigated using all-atom simulations.[123] The PG, Lys-PG, and cardiolipin (Figure 2) lipid models were employed to construct the membrane. Increased conformational flexibility was observed for lipid II in the membrane milieu. Furthermore, lipid II was prone to aggregation. The study also showed an affinity of lipid II to bind with the peptide (plectasin). A coarse-grained mimic of cytoplasmic membrane containing Ala-PG and Lys-PG was built and simulated in the Martini framework to elucidate a reduced affinity of a cationic peptide for modified lipids containing zwitterionic alanyl (Ala-PG) and cationic lysyl (Lys-PG) groups.[54] Using umbrella sampling atomistic simulations[111] with a collective variable that describes pore formation, it has been found that membranes with increased cardiolipin content are less susceptible to pore formation due to the negative curvature induced by cardiolipin.

Table 2. Literature on Cytoplasmic Inner Membrane Models for Both Gram-Positive and Gram-Negative Strains[a]

year	species	force field	lipid model
2008[34]	*E. coli*[S]	Berger lipids	PE, PG
2011[62]	*S. aureus*[S]	GROMOS53A6	PG, CL, Lys-PG
2012[106]	*E. coli*[S]	CHARMM36	PE, PG
2014[107]	*E. coli*[S]	CHARMM36	PE, PG
2015[42]	*E. coli*[S]	CHARMM36	PE, PG (cyclopropane)
2015[108]	*E. coli*[S]	GROMOS53A6, Martini	PC, PE, PG, CL
2016[109]	*E. coli*[S]	GROMOS53A6, Martini	PE, PG
2018[110]	*E. coli*, *S. aureus*[S]	CHARMM36	PE, PG
2019[57]	*B. subtilis*[S]	CHARMM36	PE, PG
2020[4]	*E. coli*[S]	CHARMM36	PE, PG, CL
2021[111]	model membranes	CHARMM36	PG, CL
2022[56]	*S. aureus*[S]	CHARMM36	PG, Lys-PG
2022[112]	*E. coli*[S]	CHARMM36	PE, PG, CL
2022[43]	*E. coli*[A]	CHARMM36	PE, PG (cyclopropane)

[a]PE, phosphatidylethanolamine; PG, phosphatidylglycerol; CL, cardiolipin; and Lys-PG, lysylphosphatidylglycerol. [A]Asymmetric bilayer. [S]Symmetric bilayer.

INTERACTIONS WITH THE OUTER MEMBRANE OF GRAM-NEGATIVE BACTERIA

It is essential to understand the molecular mechanism of permeation of small molecules through bacterial cell envelopes to develop novel antimicrobial agents, probiotics, and prebiotics. In Table 3, studies concerned with the insertion barriers for molecules in outer membrane LPS models are summarized. The outer membrane of Gram-negative bacteria acts as a strong amphiphilic barrier for small molecules because of the hydrophilic saccharides and the hydrophobic lipid tail environment.[128] The anionic LPS molecules are tightly packed due to electrostatic shielding by divalent cations (Ca^{2+} and Mg^{2+}) .[68] The slow-diffusing LPS molecules also hinder the transport of hydrophobic molecules, and the reduced lateral diffusion along the membrane plane requires sufficient sampling to reliably extract translocation free energies.[4] The bacterial membrane has evolved to act as a "semi-permeable barrier", and consequently, there are FadL channels in the outer membrane that allow for the transport of hydrophobic fatty acid molecules.[129] Similarly, small hydrophilic molecules, ions, and nutrients cross the outer membrane through pores created by outer membrane porins (OMPs).[128]

Interactions with LPS. Here we summarize the literature concerning the interactions of small molecules and ions with

https://doi.org/10.1021/acs.langmuir.3c03474
Langmuir 2024, 40, 7791−7811

Table 3. Literature on Small-Molecule Transport Studies with Gram-Negative Outer Membrane Models[a]

year	species	force field	lipid model	molecules
2008[124]	*P. aeruginosa*	GLYCAM93	Re-LPS, PE	H_2O, Cl^-, Na^+ Ca^{2+}, UO_2^{2+}
2016[99]	*E. coli*	GROMOS53A6	Re-LPS, PE	ethane, benzene
			PG, CL	hexane, ethanol, acetic acid
2016[68]	*E. coli*	Martini 2.2	Re-LPS, Ra-LPS, PE	C60 fullerene
2018[125]	*P. aeruginosa*	Martini 2.2	Ra-LPS, PE, PG	zinc compound
2019[126]	*E. coli*	Martini 2.2	Ra-LPS, PE, PG, CL	arginine
2020[4]	*E. coli*	CHARMM36	S-LPS, PE, PG, CL	thymol
2022[127]	*Pseudomonas putida*	CHARMM36	rough LPS, PE, PG	lignin derivatives

[a]LPS, lipopolysaccharide; PE, phosphatidylethanolamine; PG, phosphatidylglycerol; and CL, cardiolipin.

the LPS layer. Studies on the interactions of antimicrobial peptides are discussed in a separate section. Interestingly, one of the earliest molecular simulation studies for understanding the interactions of molecules with the outer membrane was performed to understand how microorganisms absorb contaminant metals. Lins et al.[124] utilized umbrella sampling to estimate the free energy of uptake of sodium, calcium, and chloride ions on bacterial surfaces. Due to the predominantly anionic nature of the LPS membrane, the uptake of cations was found to be energetically favorable when compared with anions, and positively charged uranyl ions exhibited a greater binding affinity to carboxyl and hydroxyl binding sites in the LPS outer core of *P. aeruginosa*.

Later, Carpenter et al.[99] utilized a united-atom model of the outer membrane and calculated the free energy of translocation for benzene, hexane, ethane, acetic acid, and ethanol, which represent a basic set of building blocks for various antimicrobials (Figure 4C). The LPS headgroup regions offered an unfavorable environment for molecules when compared with the phospholipid counterpart (Figure 4C), highlighting the need for accurate outer membrane models to understand antimicrobial translocation through the bacterial cell envelope.

Carbon fullerene finds wide applications as antibacterial agents, antioxidants, and transporters for nanosized drugs.[130] Hsu et al.[68] studied the interactions of C60 fullerene with the rough LPS outer membrane of bacteria using the Martini force field. The interactions of these molecules with the outer membrane were found to depend on the ambient temperature, phospholipid domains in the leaflet containing LPS, counterions, and length of the LPS units. Orekhov et al.[125] used a Martini model with umbrella sampling simulations to show the favorable interactions of zinc octakis(cholinyl)phthalocyanine with Ra-LPS and DPPE in the outer membrane, while for the inner membrane (POPE:POPG), a large insertion barrier was observed. The study also provides an evidence for the "self-promoted uptake"[131] of the zinc compound in the outer membrane.

Using all-atom MD simulations, Sharma et al.[4] studied the permeation of thymol, a potential antimicrobial molecule, through the smooth LPS of *E. coli* using umbrella sampling simulations. The study showed the presence of a ∼14 kJ barrier at the core saccharide region, and no translocation events were observed during 1 μs-long unbiased simulations. Thymol, however, spontaneously inserted into the phospholipid regions of both the outer and inner membranes. In recent MD simulations, membrane partitioning and permeability coefficients of lignin-related compounds have been investigated using all-atom simulations with replica exchange umbrella on rough LPS of *Pseudomonas putida*[127]. The study revealed that the core sugars offer a barrier for lignin molecules and that the energetic barrier energy increases with the hydrophobicity of the lignin compounds. Preferential binding of lignin below the lipid headgroups was observed for the inner membranes,[132] and a continuum flux model was employed to comment on membrane permeabilities at industrially relevant concentrations of lignin. A majority of the models investigated in the literature for molecule permeation through the outer membrane are predominantly with lipid A or rough LPS. Simulations with smooth LPS using a more reliable all-atom or united-atom framework are needed to gain insights into the barriers offered by O-antigen units.[4,133]

Translocation through Outer Membrane Porins (OMPs). The passage of antimicrobial molecules through the outer membrane is not always through the LPS but also through various porins and protein channels available in the outer membrane.[102] From the early all-atom simulations of the solvent-free OmpF trimeric porin[134] to porins embedded in lipids and solvent[135−137] simulated for a few nanoseconds, several insights were obtained for the role of the L3 loops, pore dimensions, ion conduction, and water density distributions. Simulations are now routinely carried out for porins in realistic asymmetric outer membrane models in all-atom and coarse-grained representations for hundreds of nanoseconds to a few microseconds with the primary focus on understanding the translocation of small molecules. Several review articles summarize the current understanding of the action and specificity of these channels[10,138] and molecular transport through them.[102] Samsudin and Khalid[126] studied arginine movement through the outer membrane using a Martini model and inferred a large barrier of ∼45 kT for the translocation of arginine through the LPS. They found that this barrier reduces significantly in outer membrane channel OprD, which provides the translocation pathway for arginine.

Bajaj et al.[140] described the electrostatic filtering mechanism of small polar molecules through OmpF using norfloxacin as a dipolar probe for this combined experimental and enhanced sampling metadynamics simulations study. The simulations were performed using a bare protein in the absence of the lipids. The translocation event involved the alignment of the molecule along the internal electric field of the channel, followed by its reorientation. The study highlighted the role of loop L3 (Figure 5) in positioning an electrostatic sieve at the physical constriction, with residues appropriately positioned to selectively allow charged molecules to transit across the pore.

Owing to the computational complexity involved in simulating bulky trimeric proteins in a realistic membrane environment, enhanced sampling techniques have been used to complement vanilla MD simulations in determining the free energy landscape of the translocation of antibiotics through porins. The lumen of most porins has a distinct region

https://doi.org/10.1021/acs.langmuir.3c03474
Langmuir 2024, 40, 7791−7811

constricted by the presence of an extracellular loop L3 (Figure 5B), which primarily acts as a constraint on the size of the molecules that can permeate through the porin (typically <600 Da). Earlier MD studies[141,142] were used to determine the free energy landscape of the translocation of ampicillin through the porin OmpF of *E. coli* using metadynamics. These studies observed the weak binding of the positively charged group of the molecule to the loop L3, suggesting it to be a temporary anchor, while the negatively charged moieties utilized a series of basic residues lining the porin wall to translocate across the porin in a sequential manner. The antibiotic had to undergo structural reorganization to overcome the barrier at this region, alluding to the significance of orientational flexibility of the molecule for its translocation. In an effort to alleviate limitations of inadequate sampling, Acharya et al.[139] combined umbrella sampling and metadynamics schemes with temperature acceleration simulations and path-based methods to determine the free energy of the translocation of ciprofloxacin in OmpF (Figure 5C,D). Importantly, the inclusion of solute degrees of freedom in the collective variable space was found to improve the reliability of the free energy computations.

Golla et al.[143] investigated the translocation of anionic molecules through the outer membrane pore OprO of *P. aeruginosa* incorporated in the atomistic model of the POPE membrane. Transport of chloride and monophosphate was found to be similar, having the same affinity site in the constricted pore region. In contrast, fosmidomycin exhibited two pathways with similar energy barriers.

Porins have been known to be a common target for mutations, enabling bacteria to acquire antimicrobial resistance. Incorporating mutated residues in porin models is a common simulation strategy to determine their effect on antibiotic translocation. Wong et al.[144] introduced mutated residues at the constriction region of OmpK36 in *Klebsiella pneumoniae*, as observed in the crystal structure from a clinically resistant strain of the bacteria. Analysis using MD simulations revealed an apparent decrease in the pore width from 3.20 to 2.37 Å at the constriction region due to these modifications, thus explaining the cause of the observed resistance. In a study by Golla et al.[145] on the translocation of the antibiotic fosfomycin across OmpF, mutating a series of basic residues at the constriction region led to an increase in the energetic barrier for antibiotic translocation.

In view of the looming threat of antimicrobial resistance, the development of new antibiotics is an urgent requirement. Using MD simulations, Dai et al.[146] recently developed a computational antibiotic screening platform (CLASP) for the in silico screening of potential antimicrobial molecules based on the thermodynamics and kinetics of their interactions with the outer membrane porin OccD3. They utilized this platform to understand the free energy barriers offered for six carbapenem antibiotics: biapenem, doripenem, ertapenem, imipenem, meropenem, and panipenem. The coarse-grained models were able to pick up the critical residues Y217A and F334A in this channel based on the high frequency contacts. The mutation of these two residues to less bulky groups significantly reduced the barrier for permeation of the carbapenem antibiotics.

Most of the studies dedicated to understand the barrier properties of the outer membrane are in the Martini framework (Table 3). Since LPS is mainly composed of sugars and the Martini 2 force field is inaccurate while modeling sugars,[97,98] the energy landscapes obtained from the Martini 2 models should be re-examined with the improved Martini 3 parametrization for sugars.[86] Hence, it requires a systematic evaluation and an improvement of interaction potentials by comparing the energy profiles with those obtained from corresponding atomistic models.[113]

INTERACTION AND TRANSLOCATION THROUGH PEPTIDOGLYCAN

Despite the extensive literature on inner and outer membrane Martini models, the translocation and interaction of molecules with peptidoglycan have only recently begun to appear in the literature. Khalid and co-workers[147] have studied the interaction of polymyxin B1 in the periplasm of *E. coli*. In order to model the crowded environment, the periplasmic space consisted of a layer of peptidoglycan, the outer Ra-LPS with Braun's lipoprotein, and several other proteins and osmolytes. Polymyxin B1 was found to bind to peptidoglycan in two modes: insertion between glycan strands, forming long-lived salt bridge interactions, and direct binding to peptide linkages. In the 500 ns simulations, polymyxin did not cross the peptidoglycan layer; however, smaller osmolytes including urea were able to translocate several times. Crowding in the periplasm resulted in up to a 100-fold decrease in the polymyxin diffusivities with crowding fraction.

Interactions of vancomycin with a POPC membrane-bound lipid II were investigated using MD simulations with the GROMOS force field.[148] Lipid II is the primary precursor molecule in the peptidoglycan synthesis pathway and a commonly used drug target. Vancomycin was found to bind spontaneously to lipid II, forming a stable complex with a peptide bond formed between the N-terminal amino group of vancomycin and the C-terminal carboxylic acid of lipid II. Free energy calculations suggested that native lipid II with D-Ala–D-Ala amino acid residues had the highest binding energy compared to the resistant and synthetic lipid II with D-Gly, D-Ser, D-Lac, and L-Ala substituents. In a similar study[149] on the interactions of peptidoglycan with vancomycin and its derivatives, layered and scaffold models of peptidoglycan were constructed and simulated using the GLYCAM all-atom force field. Using energetic conformations, a vancomycin derivative that is promising against Gram-positive infections was also identified. In another study,[150] a docking simulation was carried out on vancomycin binding to muropeptides with different termini residues. Among the complexes studied, the binding of vancomycin with muropeptide was strongest for the D-Ala–D-Ala terminated fragment. In a recent study[151] on vancomycin binding to lipid II, the importance of asparagine in the antibacterial activity of vancomycin was illustrated. A vancomycin analogue, where asparagine is substituted by aspartic acid, showed a reduction in the binding efficiency with L-Lys–D-Ala–D-Ala, confirming a crucial role of asparagine in substrate recognition.

In a recent study from our laboratory, a fully atomistic four-layered model of peptidoglycan for Gram-positive *S. aureus* was simulated to assess insertion energy barriers for thymol.[122] Thymol molecules were able to cross the cell wall over a 500 ns simulation, indicating a low energy barrier for translocation. The low barrier for thymol is consistent with observations made in an earlier Martini study of *E. coli* peptidoglycan.[113] In the same study, melittin (Figure 6A) was found to have stronger binding and penetration with the negatively charged peptidoglycan of *E. coli* when compared with the neutral *S. aureus* cell wall, and it was showed preferentially binding to D-

https://doi.org/10.1021/acs.langmuir.3c03474
Langmuir 2024, 40, 7791−7811

alanine residues implicated in the transpeptidation biosynthesis pathway.

The kinetics of surfactant (C_{12}−C_{18}) aggregation and translocation through peptidoglycan have recently been investigated using all-atom MD simulations.[112] Within the simulation time scale of 500 ns, several translocation events were reported for single-molecular transport of surfactants at different rates, and the shorter-chain laurate showed the highest number of translocation events when compared with other long-chain surfactants. The kinetics of aggregation for laurate were slow on account of it having a relatively higher critical concentration for micellar aggregation, and consequently, the laurate molecules were able to translocate more efficiently when compared with the long-chain stearate and oleate molecules. The results of the study correlated well with bacterial kill data kinetics, showing that the antibacterial activity of surfactants is governed by the availability of free surfactants and their translocation kinetics, which are a function of the chemistry of the specific surfactant.

■ SURFACTANTS AS ANTIMICROBIALS

Surfactants are widely used in personal care formulations due to their antimicrobial properties.[152] Although surfactants are known to solubilize the cell membrane,[153] the underlying molecular mechanisms for bacterial kill remain elusive. The complex membrane solubilization mechanism depends on the physicochemical properties of the surfactant, surfactant concentration, and thermodynamic phase state of the lipid membrane.[154] Several experimental[153] and simulations studies have been dedicated to understanding the interactions of surfactants with lipid bilayers. The three-stage model proposed by Helenius and Simons[155] attempts to explain the mechanism of membrane solubilization[154] by surfactants. In the first stage, the surfactant partitions into the lipid bilayer until saturation is reached. The next stage is characterized by perturbation of the bilayer structure, resulting in the formation of mixed micelles of surfactants and lipids. A further increase in the surfactant concentration results in membrane solubilization and the formation of smaller mixed micelles, which are eventually dispersed in the solvent. Although the three-stage model provides a mechanistic view for the solubilization of lipid bilayers, the extension to the other bacterial membrane components is unclear.

With the exception of a recent study from our laboratory,[4] where surfactant interactions with the bacterial plasma membrane were studied, surfactant−membrane studies have been largely restricted to interactions with the plasma membrane. We, however, briefly review this literature, as it is relevant to our understanding of the interactions of surfactants with the bacterial cell envelope.

Using a united-atom GROMOS force field, Xu et al.[156] found that sodium dodecyl sulfate (SDS) molecules readily partitioned into a DPPC bilayer with the carbon tails oriented along the lipid tails, resulting in a decrease in the bilayer area and an increase in thickness. In early all-atom studies with surfactant-incorporated plasma membranes, the influence on lipid ordering and other membrane properties has also been studied.[157,158]

Groot and Rabone[159] used coarse-grained dissipative particle dynamics (DPD) models[160] to recognize the origin of bacterial cell death when exposed to surfactants. Bilayer models with PE lipids were built with surfactants $C_{12}E_6$ and C_9E_8 at varying concentrations. $C_{12}E_6$ was found to efficiently form transmembrane pores only at very high surfactant concentrations (>90%), while transient pores were observed even at lower concentrations for C_9E_8. The study revealed that surfactant incorporation reduced the extensibility and stress bearing capability of the membrane.

Huang et al.[161] studied the interactions of surfactants with lipid vesicles using DPD models. Corroborating the three-stage mechanism of membrane solubilization, the structure of lipid assembly was observed to change from stable vesicles to distorted vesicles coexisting with mixed micelles composed of lipids and surfactants at varying concentrations of surfactant. The vesicles were solubilized to mixed micelles at high surfactant concentrations. The correlations between the hydrophobic character of the surfactant and its partitioning into the lipid assembly were also established. Later, Lin et al.[162] adopted the same DPD models and extended the study to show that vesicle solubilization occurred in the presence of surfactants with optimum hydrophobicity. Surfactants with low hydrophobicity could not partition into the vesicles and preferred to remain in solution, leaving the vesicles unaffected. In comparison, the surfactants with extreme hydrophobicity partitioned into the vesicle and increased its size. Interestingly, for these surfactants, vesicles reshaped into cylinders, donuts, and bilayers. It was concluded that the process of vesicle solubilization with surfactants is more complex than that posited by the three-stage hypothesis. Martini simulations were also explored to shed light on lipid−surfactant interactions. With DPPC lipid and Triton TX-100 surfactant, Martini constructs for monolayers and bilayers were developed and simulated.[163] The area per surfactant was found to be in good agreement with experimental results.[164] Due to hydrophilic chains, Triton TX-100 domains in the lipid membrane induced local curvature. In another study by Pizzirusso et al.,[154] the distinct pathways that rely on the kinetics of surfactant partitioning were elucidated for membrane solubilization.

Surfactant (C_{12}−C_{18})-incorporated bacterial membranes were studied using all-atom MD simulations in our recent work.[112] The membrane properties were found to be perturbed to a greater extent by short-chain laurate molecules in comparison to long-chain oleate and stearate molecules. Laurate molecules in the bacterial membrane resulted in greater hydrophobic mismatch and membrane thinning, and the laurate-mixed membrane was more prone to poration under electric fields compared to the membranes containing longer-chain surfactants. Interestingly, the greater perturbation with the laurate surfactants correlated well with the rapid contact time kill efficacy data from experimental studies on *E. coli*.[112]

■ TRANSLOCATION OF ANTIMICROBIAL PEPTIDES

Antimicrobial peptides (AMPs) are a class of synthetic or naturally occurring peptides containing 10−60 amino acid residues that are ubiquitously found in microbes, insects, plants, animals, and humans. The translocation of AMPs across the bacterial membrane has been the subject of several MD simulation studies.[165] Generally, AMPs are amphipathic, exhibit great variability in sequence, and possess a net positive charge to increase interactions with the negatively charged bacterial outer and inner membranes. Actions of AMPs include membrane binding, permeation, secondary structure changes, and oligomerization to form pores that result in bacterial cell lysis. The pathways will depend on both the peptide and the bacterial strains.[166,167] Circular dichroism, cryo-electron

https://doi.org/10.1021/acs.langmuir.3c03474
Langmuir 2024, 40, 7791−7811

microscopy, and NMR measurements are some of the experimental techniques employed to study the structural changes and membrane perturbations that occur during the interaction and penetration of AMPs in membranes.[166,167] Here, we focus on simulation studies concerned with the interaction of AMPs with predominantly anionic bacterial outer and inner membranes. Tables 4 and 5 provide a summary of the relevant literature.

Table 4. Literature on Antimicrobial Peptide Interactions with Symmetric Inner Membrane Models[a]

year	force field	lipid model	peptide
2012[168]	CHARMM36	PG, PC	CM15
2016[166]	CHARMM36	PE, PG	magainin 2
2016[169]	CHARMM27, Slipids	PE, PG	CM15
2018[171]	Martini 2.2p	PE, PG	aurein 1.2
2018[177]	CHARMM36	PE, PG	magainin 2
2018[178]	GROMOS53A6 Kukol	DMPG	daptomycin
2018[179]	GROMOS54A7 Kukol	PG, CL	aurein 1.2
2020[176]	CHARMM36m	DPPE, DPPG	GF17
2020[167]	CHARMM36	PE, PG	LL37
2021[54]	Martini 3	PE, PG, Lys-PG	amhelin, magainin 2
2022[172]	CHARMM36	PE, PG	LL37
2024[170]	CHARMM36	PC, PE	transportan-10

[a]PE, phosphatidylethanolamine; PG, phosphatidylglycerol; CL, cardiolipin; DPPG, dipalmitoylphosphatidylglycerol; DPPE, 1,2-dipalmitoyl-*sn*-glycero-3-phosphoethanolamine; DMPG, 1,2-dimyristoyl-*sn*-glycero-3-phosphoglycerol; PC, phosphatidylcholine; and Lys-PG, lysylphosphatidylglycerol.

Table 5. Literature on Antimicrobial Peptide Translocation across Bacterial Asymmetric Outer Membrane Models[a]

year	force field	lipid model	peptide
2015[180]	GROMOS53A6, Martini 2	Re-LPS, PE, PG	polymyxin
2017[182]	GROMOS53A6	mutant LPS, PE, PG	polymyxin
2022[183]	CHARMM36	Re-LPS, PE, PG, CL	polymyxin
2022[184]	CHARMM36m, Martini 2.2	Re-LPS, PE, PG, CL	adepantin-1
2022[185]	CHARMM36m, Martini 2.2p	lipid A, PE, PG, CL	AMPR11, AMPR22
2022[186]	CHARMM36	Re-LPS, PE, PG, CL	CM15

[a]LPS, lipopolysaccharide; PE, phosphatidylethanolamine; PG, phosphatidylglycerol; and CL, cardiolipin.

Using MD simulations, Wang et al.[168] studied the influence of initial states (random coil and α-helical) of CM15 peptide (KWKLFKKIGAVLKVL, a synthetic AMP derived from cecropin A and melittin) on its conformational changes while interacting with POPC and POPC:POPG model membranes. CM15 showed preferential binding with anionic PG lipids through electrostatic interactions when compared with a pure POPC membrane. Moreover, a CM15 peptide with a random coil configuration exhibited enhanced electrostatic interactions compared to a prefolded α-helical peptide, indicating the influence of peptide secondary structure on peptide−membrane interactions. The study, therefore, indicates that both the charge state of the membrane and the secondary structure adopted by the peptide are important factors that influence the antimicrobial activity of the peptide.

A simulation study by Bennett et al.[169] on CM15-induced pore formation on phospholipid membranes showed the differences in free energy barriers with Berger, Slipids, and CHARMM36 force fields. In particular, the Berger and Slipids force fields showed a lower barrier for pore formation when compared with the CHARMM36 force field. Membrane properties, such as the membrane thickness and area per lipid, were found to be force field dependent, leading to differences in the free energy barriers. For instance, by reducing the van der Waal's cutoff in the CHARMM36 force field, the membrane thickness decreased, in turn reducing the free energy barrier for pore formation. Additionally, pore formation was found to be sensitive to the treatment of electrostatic interactions. A reduction in the free energy barrier was observed using the reaction field method. This study further illustrates that the simulation results from different force fields on a lipid membrane can be compared once structural properties of the membrane are suitably normalized. In a recent MD study on the interaction of the cell-penetrating peptide transportan-10 in POPC bilayers, CHARMM36 force field was found to stabilize the helical state of the membrane-inserted peptide when compared with the GROMOS and OPLS-AA force fields.[170] However, the accuracy of a given force field would depend on comparisons made with available experimental data. These vanilla MD simulations suggest that a larger collective variable space is needed while studying membrane−peptide interactions. Collective variables include the distance along the bilayer normal, the angle with the normal, and the secondary structure changes that occur during membrane insertion. Umbrella sampling simulations using the distance along the membrane normal as the collective variable with transportan-10W (AGWLLGKINLKALAALAKKIL-NH2), a 21 residue cationic peptide, on POPC model membranes showed the presence of two minima: one for the surface-bound state and the other for the vertically oriented membrane-inserted state.[170] A detailed comparative study using different force fields (CHARMM36, GROMOS53A6, GROMOS43A2, GROMOS87, and OPLS-AA) of the secondary structure transition on the membrane showed that the CHARMM36 force field provided the closest correspondence with experimental observations.[170]

Coarse-grained Martini simulation studies of α-helical peptides, namely aurein 1.2 (GLFDIIKKIAESFNH2) and maculatin 1.1 (GLFGVLAKVAAHVVPAIAEHFNH2), were completed using pre-inserted initial states in POPG:POPE bilayers. Both peptides formed transmembrane aggregates; however, pore formation was observed for aurein 1.2, which showed deeper insertion into the membrane.[171] The mechanistic model describing the lytic action mechanism of LL37, a human antimicrobial peptide secreted as part of the innate immune response, in a POPE:POPG (3:1) bacterial membrane has been proposed using the observations from combined circular dichroism, cryo-electron microscopy, and MD simulations. This study highlighted the importance of electrostatic interactions of LL37 with the outer LPS and the oligomerization of LL37 to form channels inside the inner membrane to cause cell disruption by forming a water channel.[167] The membrane-inserted LL37 remained in a helical form, and the structural flexibility of LL37 in different physiological conditions was shown to mediate peptide interactions to initiate membrane disruption. Atomistic MD simulations of LL37 with vitamin B3 analogues such as niacinamide, *N*-methylnicotinamide, and isonicotinamide on a

https://doi.org/10.1021/acs.langmuir.3c03474
Langmuir 2024, 40, 7791−7811

pure DPPG membrane showed that synergistic effects enhance the effectiveness of peptides by decreasing the thickness and membrane rigidity.[172]

Using MD simulations,[110] GF17 peptide (FKRIVQ-RIKDFLRNLV) interactions on Gram-positive (ratio 1:3 of PE:PG) and Gram-negative (ratio 3:1 of PE:PG) membranes showed that lysine and arginine residues interact with the headgroups of the lipid membranes through hydrogen bonds and electrostatic interactions. These results agreed with NMR spectroscopy experiments, wherein arginine formed atomic contacts with PG lipids.[173] Phenylalanine had stronger interactions with the acyl chains, resulting in greater insertion into the hydrophobic core of the membrane.[174] Despite the short 300 ns simulations, the peptide was found to adopt a stable helical structure upon binding to the membrane surface. The depth of penetration of the cationic residues was restricted to the membrane surface due to the salt bridges between the cationic residues and phosphorus atoms, while the hydrophobic residues such as asparagine, leucine, and valine were able to access the hydrophobic membrane core due to favorable phenylalanine interactions. The energetic interactions of the peptide were contrasted between *E. coli* and *S. aureus* membranes. The polar interactions of the peptide with the *S. aureus* membrane were much stronger than those with the *E. coli* membrane due to the higher content of anionic PG lipids. This observation is consistent with experimental studies showing the higher efficacy of G17 in killing *S. aureus* when compared with *E. coli* strains.[175] In summary, (i) cationic peptides would show higher antimicrobial efficacy for bacterial membranes that have higher anionic lipid content. (ii) Polar residues bind strongly to the lipid headgroups, enhancing the initial binding of the peptide, and (iii) the hydrophobic residues increase the depth of peptide penetration, eventually leading to membrane rupture.

In another study[176] on the interactions of GF17 with bacterial membranes composed of PE and PG lipids, it was found that the membrane area and lipid mobility increased upon peptide binding, and the interactions were energetically more favorable with the pure PG membrane compared to PE:PG membranes. The peptide adopted α-helical and coil structures in the membrane milieu, and the peptide structures were observed to be more compact and less flexible in the pure PG membrane.

In order to unravel the underlying mechanism of the antibacterial action of pleurocidin (GWGSFFKKAAHVGKHVGKAALTHYLNH2) and magainin 2 (GIGKFLHSAKK-FGKAFVGEIMNSNH2) on Gram-negative strains, NMR experiments and MD simulation studies were carried out on a POPE:POPG (3:1) bilayer.[166] Despite having physical and structural similarities, these peptides exhibit dramatically different antimicrobial activity on bacterial membranes. Both peptides have a similar length of amino acid residues, hydrophobic content, hydrophobic moment in α-helical structures and charge. Pleurocidin has greater conformational flexibility, allowing for deeper membrane penetration, while magainin 2 penetrates into the membrane only at higher peptide-to-lipid ratios. The relatively greater disordered conformation of pleurocidin resulted in higher antibacterial activity when compared to magainin 2. In the NMR studies, magainin 2 had a pronounced kink at G-13, creating two distinct helical regions in the peptide, while a pronounced distortion of helix was observed between S-4 and G-13 in pleurocidin. Another key difference observed in the NMR structures of these peptides was that the distortion of helix at G-18 in magainin 2 was less pronounced compared to the distortion in the helical structure at G-17 in pleurocidin.

Enhanced umbrella sampling simulations of magainin 2 (a natural peptide) on *E. coli* membranes (POPE:POPG in a ratio of 3:1) have shown that the aggregates of magainin 2 induced by guanine units attached to the peptides had a higher free energy for insertion when compared with a single peptide.[177] This study indicates that peptide aggregation is detrimental to membrane binding and penetration.[177] Increased susceptibility of anionic membranes to cationic peptides has been demonstrated in a peptide−membrane study,[178] where a higher free energy of insertion for daptomycin in DMPE:DMPG mixed membranes was observed compared with a pure DMPE membrane.

Although cardiolipin is present in varying concentrations in the bacterial inner membrane and increased cardiolipin is implicated in resistance, very few studies have examined the influence of cardiolipin on peptide binding, insertion, and antimicrobial activity. A study using 200 ns MD simulations with aurein 1.2 (GLFDIIKKIAESFNH2) on POPG:CL (70:30) membranes revealed a strong membrane buckling phenomenon with increased aurein 1.2 concentrations.[179] The peptide was surface-bound with helical content independent of the peptide concentration.

We next review the literature on AMP interactions with the LPS membrane of Gram-negative bacteria. Using the GROMOS force field, MD simulations[180] with Re-LPS showed that polymyxin B1 was able to interact with phosphate groups present in the sugars, displacing magnesium ions in the LPS region. Binding of the γ-diamino butyric acid moiety in polymyxin B1 was dominant. Simulations with the inner membrane made up of DOPE:DOPG:CL (75:25:5) showed strong binding and acyl chain insertion into the lipid region. A coarse-grained Martini study by Jefferies et al.[181] showed that the presence of polymyxin B1 resulted in an increase in the crystalline states of LPS. The peptide modified the LPS dynamics by decreasing the translational entropy, particularly in the phosphate-containing regions.

Studies of polymyxin B binding and interactions with lipid A and Re-LPS from both resistant and susceptible bacterial strains have shown increased membrane curvature induced due to polymyxin B binding for the susceptible strains and an overall enhancement of calcium ion diffusivities.[182] A detailed study on the energetics of polymyxin interactions with LPS molecules for mutant strains of *P. aeruginosa* revealed the differences in free energy barriers with a greater barrier for insertion in the mutants when compared with the wild type LPS and Re-LPS.[183] The study also showed the interactions of hydrophobic fatty acyl group and leucine residues in assisting the conformational folding of polymyxin in the outer membranes. Binding modes of adepantin-1 onto the model membranes for Gram-positive and Gram-negative membranes have been studied using all-atom and coarse-grained simulations. The importance of lysine residues in peptide−membrane interactions was highlighted.[184] Understanding the lipid-mediated changes in peptide conformation is an important aspect in the design of synthetic peptides. In a study on AMPR11 and AMPR22 interacting with bacterial inner membranes, it was observed that AMPR22 adopted greater helicity by forming hydrogen bonds with cardiolipin.[185] On account of the heterogeneity in the chemical structure of bacterial outer membrane LPS molecules, the insertion barriers

https://doi.org/10.1021/acs.langmuir.3c03474
Langmuir 2024, 40, 7791−7811

for antimicrobial peptides show variability across different regions of LPS. Free energy landscapes determined by Sharma and Ayappa for the antimicrobial peptide CM15[186] using umbrella sampling simulations indicated spontaneous penetration into the O-antigen region with a large barrier in the core saccharide region. Secondary structure changes showed that the peptide prefers to remain unfolded in the core saccharide region.

From the reported studies, it can be inferred that there are several challenges involved while investigating the translocation of antimicrobials across the bacterial membrane. A judicious choice of the force field is crucial, and several studies have investigated the variation in the conformational[169] and thermodynamic behavior[170] of peptides in the membrane environment with different force fields. This raises a different set of challenges, and the accuracy of the force fields requires validation with experimental observations. It is important to note that several microsecond-long MD simulations must be used to draw reliable conclusions from restraint-free computations. Another ongoing challenge is the choice of collective variables to evaluate the free energy landscape. In addition to the center-of-mass distance between the membrane and the peptides, which has widely been used, it is important to study the free energy with respect to other collective variables that influence peptide−membrane interactions. Some of the collective variables during peptide pore formation include the secondary structural transition of the peptide, peptide hydration, and the translocation of phosphorus headgroups leading to flip-flop events in the membrane. Few computational techniques, such as the string method,[187] have been recently used in free energy estimations involving path collective variables. This is an ongoing area of research, and advanced sampling methods are needed to capture the complete free energy landscape associated with peptide−membrane binding events.

CONCLUSION AND PERSPECTIVES

To complement standard drug discovery tools, a molecular-level understanding of the interactions of potential drug candidates with the complex architecture of cell envelopes of bacterial pathogens is crucial. In this regard, MD simulations have evolved as a powerful in silico platform to aid in the selection and screening of potential drug and antimicrobials. The success of this approach depends on the accuracy of interactions used in the molecular models and continuous reliability assessment with appropriate experimental data. A detailed understanding of the specific molecular interactions and transport of antibacterial therapeutics with the bacterial cell envelope will also facilitate drug molecule development to combat the emergence of drug-resistant strains. In this review, we have provided an overview of several key MD simulation results that have led to an improved understanding of interactions with the different membrane components of both Gram-positive and Gram-negative strains. Our review follows the development of molecular models of the various components in the cell envelope to reveal the wealth of detailed information that can be obtained using MD simulation studies.

Apart from the structural aspects of the bacterial cell envelope, this review lays emphasis on the interactions of small molecules, antimicrobials, surfactants, and AMPs with the cell envelope. Recent additions to the literature on peptidoglycan model development for both Gram-positive and Gram-negative strains as well as attempts to model the complex landscape of the periplasm have been addressed. We have not discussed literature concerning the transmembrane protein machinery involved in lipid transport and folding as well as efflux pump action, and recent reviews[188,189] cover the literature in this field.

Although there is a notable increase in the number of studies on the transport of small molecules through different compartments of the bacterial cell envelope, several challenges remain. The first is a complete description of the collective variable space to describe the free energy landscapes for molecule translocation, which is more complex in the case of proteins and antimicrobial peptides. In addition to the depth of penetration, rotational degrees of freedom and secondary structure changes that occur during membrane insertion need to be included as collective variables.[190] There is also a need to use more accurate inner membrane compositions that correspond to the bacterial membranes of Gram-positive and Gram-negative strains. When secondary structure changes are involved, appropriate coarse-grained methods that reliably capture unfolding and refolding events[187,191] should be used to obtain the free energy landscape. Appropriately parametrized coarse-grained membrane and sugar representations would be required to capture translocation through the outer membrane and peptidoglycan environments. Improvements in the sugar interaction force fields in the latest Martini 3 models do address this aspect, allowing for improved Martini-based representations, as shown in our recent work of the Gram-negative outer membrane.[79] Studies assessing the translocation free energies of molecules using these outer membrane models have yet to appear in the literature.

Despite the growing MD simulations literature, several aspects of the bacterial cell envelope need attention. These include (i) the development of models for the peptidoglycan of Gram-positive strains with teichoic acids and their influence on interactions with external molecules, (ii) increased attention to the periplasm, which plays a critical role in transporting proteins from the cytosol to the outer membrane environment, (iii) understanding protein folding in the outer membrane, (iv) the transport of molecules under varying stress conditions experienced by bacteria, and (v) mechanisms of efflux pump action. An area that is less studied partly due to the inherent compositional complexity of using MD simulations is the structure of biofilms primarily made up of polysaccharides. Simulations are likely to provide insights into ways to prevent biofilm formation and to understand the transport of antimicrobials through the biofilm. With advances in cryo-EM techniques and super-resolution single-molecule fluorescence-based microscopy, both structural and dynamical aspects of the bacterial cell envelope will be studied with greater resolution.[192] Improvements in enhanced sampling and coarse-grained protocols will allow MD simulations to play a significant role in our understanding of processes that occur in the complex landscape of the bacterial cell envelope, opening a wider space for the design of ecologically benign antimicrobials and novel next-generation therapeutics for bacterial infections.

AUTHOR INFORMATION

Corresponding Author

K. Ganapathy Ayappa − *Department of Chemical Engineering, Indian Institute of Science, Bangalore, Karnataka, India*

https://doi.org/10.1021/acs.langmuir.3c03474
Langmuir 2024, 40, 7791−7811

560012; orcid.org/0000-0001-7599-794X; Email: ayappa@iisc.ac.in

Authors

Pradyumn Sharma − *Department of Chemical Engineering, Indian Institute of Science, Bangalore, Karnataka, India 560012;* Present Address: Eli Lilly Services India Private Limited, Bangalore 560103, India; orcid.org/0000-0002-4489-1832

Rakesh Vaiwala − *Department of Chemical Engineering, Indian Institute of Science, Bangalore, Karnataka, India 560012;* orcid.org/0000-0003-1862-8659

Amar Krishna Gopinath − *Department of Chemical Engineering, Indian Institute of Science, Bangalore, Karnataka, India 560012*

Rajalakshmi Chockalingam − *Department of Chemical Engineering, Indian Institute of Science, Bangalore, Karnataka, India 560012;* orcid.org/0000-0001-7199-9809

Complete contact information is available at: https://pubs.acs.org/10.1021/acs.langmuir.3c03474

Author Contributions

¶P.S. and R.V. contributed equally to this work.

Notes

The authors declare no competing financial interest.

■ ACKNOWLEDGMENTS

R.V. acknowledges Unilever Research and Development (Bengaluru, India) for the financial support, and R.C. acknowledges the support from the Indian Institute of Science under the Institute of Eminence postdoctoral fellowships. The authors also acknowledge the Science and Engineering Research Board (SERB) India for the financial support.

■ REFERENCES

(1) Yu, Z.; Qin, W.; Lin, J.; Fang, S.; Qiu, J. Antibacterial mechanisms of polymyxin and bacterial resistance. *Biomed. Res. Int.* **2015**, *2015*, 679109.
(2) Choi, H.; Yang, Z.; Weisshaar, J. C. Single-cell, real-time detection of oxidative stress induced in Escherichia coli by the antimicrobial peptide CM15. *Proc. Natl. Acad. Sci. U.S.A.* **2015**, *112*, E303−E310.
(3) Marrink, S. J.; Corradi, V.; Souza, P. C.; Ingólfsson, H. I.; Tieleman, D. P.; Sansom, M. S. Computational modeling of realistic cell membranes. *Chem. Rev.* **2019**, *119*, 6184−6226.
(4) Sharma, P.; Parthasarathi, S.; Patil, N.; Waskar, M.; Raut, J. S.; Puranik, M.; Ayappa, K. G.; Basu, J. K. Assessing barriers for antimicrobial penetration in complex asymmetric bacterial membranes: A case study with thymol. *Langmuir* **2020**, *36*, 8800−8814.
(5) Ingólfsson, H. I.; Melo, M. N.; van Eerden, F. J.; Arnarez, C.; Lopez, C. A.; Wassenaar, T. A.; Periole, X.; de Vries, A. H.; Tieleman, D. P.; Marrink, S. J. Lipid Organization of the Plasma Membrane. *J. Am. Chem. Soc.* **2014**, *136*, 14554−14559.
(6) Macháň, R.; Hof, M. Lipid diffusion in planar membranes investigated by fluorescence correlation spectroscopy. *BBA-Biomembranes* **2010**, *1798*, 1377−1391.
(7) Semeraro, E. F.; Marx, L.; Frewein, M. P.; Pabst, G. Increasing complexity in small-angle X-ray and neutron scattering experiments: from biological membrane mimics to live cells. *Soft Matter* **2021**, *17*, 222−232.
(8) Harkewicz, R.; Dennis, E. A. Applications of mass spectrometry to lipids and membranes. *Annu. Rev. Biochem.* **2011**, *80*, 301−325.
(9) Stone, M. B.; Shelby, S. A.; Veatch, S. L. Super-resolution microscopy: shedding light on the cellular plasma membrane. *Chem. Rev.* **2017**, *117*, 7457−7477.
(10) Im, W.; Khalid, S. Molecular Simulations of Gram-Negative Bacterial Membranes Come of Age. *Annu. Rev. Phys. Chem.* **2020**, *71*, 171−188.
(11) Gumbart, J. C.; Beeby, M.; Jensen, G. J.; Roux, B. Escherichia coli peptidoglycan structure and mechanics as predicted by atomic-scale simulations. *PLoS Comput. Biol.* **2014**, *10*, No. e1003475.
(12) Miller, S. I.; Salama, N. R. The gram-negative bacterial periplasm: Size matters. *PLoS Biol.* **2018**, *16*, No. e2004935.
(13) Poole, K. Multidrug resistance in Gram-negative bacteria. *Curr. Opin. Microbiol.* **2001**, *4*, 500−508.
(14) May, K. L.; Grabowicz, M. The bacterial outer membrane is an evolving antibiotic barrier. *Proc. Natl. Acad. Sci. U.S.A.* **2018**, *115*, 8852−8854.
(15) Li, A.; Schertzer, J. W.; Yong, X. Molecular dynamics modeling of Pseudomonas aeruginosa outer membranes. *Phys. Chem. Chem. Phys.* **2018**, *20*, 23635−23648.
(16) Rossi, R. M.; Yum, L.; Agaisse, H.; Payne, S. M. Cardiolipin synthesis and outer membrane localization are required for Shigella flexneri virulence. *mBio* **2017**, *8*, e01199-17.
(17) Erridge, C.; Bennett-Guerrero, E.; Poxton, I. R. Structure and function of lipopolysaccharides. *Microbes. Infect.* **2002**, *4*, 837−851.
(18) Kuhn, H.-M.; Meier-Dieter, U.; Mayer, H. ECA, the enterobacterial common antigen. *FEMS Microbiol. Rev.* **1988**, *54*, 195−222.
(19) Whitfield, C. Biosynthesis and assembly of capsular polysaccharides in Escherichia coli. *Annu. Rev. Biochem.* **2006**, *75*, 39−68.
(20) Dramsi, S.; Magnet, S.; Davison, S.; Arthur, M. Covalent attachment of proteins to peptidoglycan. *FEMS Microbiol. Rev.* **2008**, *32*, 307−320.
(21) Braun, V. Covalent lipoprotein from the outer membrane of Escherichia coli. *BBA-Rev. Biomembr.* **1975**, *415*, 335−377.
(22) Gan, L.; Chen, S.; Jensen, G. J. Molecular organization of Gram-negative peptidoglycan. *Proc. Natl. Acad. Sci. U.S.A.* **2008**, *105*, 18953−18957.
(23) Matias, V. R.; Beveridge, T. J. Cryo-electron microscopy reveals native polymeric cell wall structure in Bacillus subtilis 168 and the existence of a periplasmic space. *Mol. Microbiol.* **2005**, *56*, 240−251.
(24) Matias, V. R.; Beveridge, T. J. Native cell wall organization shown by cryo-electron microscopy confirms the existence of a periplasmic space in Staphylococcus aureus. *J. Bacteriol.* **2006**, *188*, 1011−1021.
(25) Matias, V. R.; Al-Amoudi, A.; Dubochet, J.; Beveridge, T. J. Cryo-transmission electron microscopy of frozen-hydrated sections of Escherichia coli and Pseudomonas aeruginosa. *J. Bacteriol.* **2003**, *185*, 6112−6118.
(26) Yao, X.; Jericho, M.; Pink, D.; Beveridge, T. Thickness and elasticity of gram-negative murein sacculi measured by atomic force microscopy. *J. Bacteriol.* **1999**, *181*, 6865−6875.
(27) Braun, V.; Gnirke, H.; Henning, U.; Rehn, K. Model for the structure of the shape-maintaining layer of the Escherichia coli cell envelope. *J. Bacteriol.* **1973**, *114*, 1264−1270.
(28) Wientjes, F.; Woldringh, C.; Nanninga, N. Amount of peptidoglycan in cell walls of gram-negative bacteria. *J. Bacteriol.* **1991**, *173*, 7684−7691.
(29) Oldmixon, E.; Glauser, S.; Higgins, M. Two proposed general configurations for bacterial cell wall peptidoglycans shown by space-filling molecular models. *Biopolymers* **1974**, *13*, 2037−2060.
(30) Glauner, B.; Höltje, J.; Schwarz, U. The composition of the murein of Escherichia coli. *J. Biol. Chem.* **1988**, *263*, 10088−10095.
(31) Harz, H.; Burgdorf, K.; Höltje, J.-V. Isolation and separation of the glycan strands from murein of Escherichia coli by reversed-phase high-performance liquid chromatography. *Anal. Biochem.* **1990**, *190*, 120−128.
(32) Costa, K.; Bacher, G.; Allmaier, G.; Dominguez-Bello, M. G.; Engstrand, L.; Falk, P.; de Pedro, M. A.; García-del Portillo, F. The

morphological transition of Helicobacter pylori cells from spiral to coccoid is preceded by a substantial modification of the cell wall. *J. Bacteriol.* **1999**, *181*, 3710−3715.
(33) Hayhurst, E. J.; Kailas, L.; Hobbs, J. K.; Foster, S. J. Cell wall peptidoglycan architecture in Bacillus subtilis. *Proc. Natl. Acad. Sci. U.S.A.* **2008**, *105*, 14603−14608.
(34) Zhao, W.; Róg, T.; Gurtovenko, A. A.; Vattulainen, I.; Karttunen, M. Role of phosphatidylglycerols in the stability of bacterial membranes. *Biochimie* **2008**, *90*, 930−938.
(35) Romantsov, T.; Guan, Z.; Wood, J. M. Cardiolipin and the osmotic stress responses of bacteria. *BBA-Biomembr.* **2009**, *1788*, 2092−2100.
(36) Carranza, G.; Angius, F.; Ilioaia, O.; Solgadi, A.; Miroux, B.; Arechaga, I. Cardiolipin plays an essential role in the formation of intracellular membranes in Escherichia coli. *BBA-Biomembr.* **2017**, *1859*, 1124−1132.
(37) Zaeifi, D.; Najafi, A.; Mirnejad, R. Molecular Dynamics Simulation of Antimicrobial Peptide CM15 in Staphylococcus Aureus and Escherichia coli Model Bilayer Lipid. *Iran. J. Biotechnol.* **2023**, *21*, No. e3344.
(38) Mileykovskaya, E.; Dowhan, W. Visualization of phospholipid domains in Escherichia coli by using the cardiolipin-specific fluorescent dye 10-N-nonyl acridine orange. *J. Bacteriol.* **2000**, *182*, 1172−1175.
(39) Gidden, J.; Denson, J.; Liyanage, R.; Ivey, D. M.; Lay Jr, J. O. Lipid compositions in Escherichia coli and Bacillus subtilis during growth as determined by MALDI-TOF and TOF/TOF mass spectrometry. *Int. J. Mass Spectrom.* **2009**, *283*, 178−184.
(40) Kocsis, B.; Kilár, A.; Péter, S.; Dörnyei, Á.; Sándor, V.; Kilár, F. Mass spectrometry for profiling LOS and lipid A structures from whole-cell lysates: directly from a few bacterial colonies or from liquid broth cultures. *Methods Mol. Biol.* **2017**, *1600*, 187−198.
(41) Dufourc, E. J.; Smith, I. C.; Jarrell, H. C. The role of cyclopropane moieties in the lipid properties of biological membranes: a deuterium NMR structural and dynamical approach. *Biochemistry* **1984**, *23*, 2300−2309.
(42) Khakbaz, P.; Klauda, J. B. Probing the importance of lipid diversity in cell membranes via molecular simulation. *Chem. Phys. Lipids* **2015**, *192*, 12−22.
(43) Hsieh, M.-K.; Klauda, J. B. Leaflet Asymmetry Modeling in the Lipid Composition of Escherichia coli Cytoplasmic Membranes. *J. Phys. Chem. B* **2022**, *126*, 184−196.
(44) Beeby, M.; Gumbart, J. C.; Roux, B.; Jensen, G. J. Architecture and assembly of the Gram-positive cell wall. *Mol. Microbiol.* **2013**, *88*, 664−672.
(45) Weidenmaier, C.; Peschel, A. Teichoic acids and related cell-wall glycopolymers in Gram-positive physiology and host interactions. *Nat. Rev. Microbiol.* **2008**, *6*, 276−287.
(46) Vollmer, W.; Seligman, S. J. Architecture of peptidoglycan: more data and more models. *Trends Microbiol.* **2010**, *18*, 59−66.
(47) Snowden, M. A.; Perkins, H. R. Peptidoglycan cross-linking in Staphylococcus aureus: An apparent random polymerisation process. *Eur. J. Biochem.* **1990**, *191*, 373−377.
(48) Boneca, I. G.; Huang, Z.-H.; Gage, D. A.; Tomasz, A. Characterization of Staphylococcus aureus cell wall glycan strands, evidence for a new β-N-acetylglucosaminidase activity. *J. Biol. Chem.* **2000**, *275*, 9910−9918.
(49) Hughes, R. Autolysis of Bacillus cereus cell walls and isolation of structural components. *Biochem. J.* **1971**, *121*, 791−802.
(50) Warth, A.; Strominger, J. Structure of the peptidoglycan from vegetative cell walls of Bacillus subtilis. *Biochemistry* **1971**, *10*, 4349−4358.
(51) Ward, J. B. The chain length of the glycans in bacterial cell walls. *Biochem. J.* **1973**, *133*, 395.
(52) Kaneda, T. Iso-and anteiso-fatty acids in bacteria: biosynthesis, function, and taxonomic significance. *Microbiol. Rev.* **1991**, *55*, 288−302.
(53) Oku, Y.; Kurokawa, K.; Ichihashi, N.; Sekimizu, K. Characterization of the Staphylococcus aureus mprF gene, involved in lysinylation of phosphatidylglycerol. *Microbiology* **2004**, *150*, 45−51.
(54) Simcock, P. W.; Bublitz, M.; Cipcigan, F.; Ryadnov, M. G.; Crain, J.; Stansfeld, P. J.; Sansom, M. S. Membrane binding of antimicrobial peptides is modulated by lipid charge modification. *J. Chem. Theory Comput.* **2021**, *17*, 1218−1228.
(55) Malanovic, N.; Lohner, K. Gram-positive bacterial cell envelopes: The impact on the activity of antimicrobial peptides. *BBA-Biomembr.* **2016**, *1858*, 936−946.
(56) Joodaki, F.; Martin, L. M.; Greenfield, M. L. Generation and Computational Characterization of a Complex Staphylococcus aureus Lipid Bilayer. *Langmuir* **2022**, *38*, 9481−9499.
(57) Mostofian, B.; Zhuang, T.; Cheng, X.; Nickels, J. D. Branched-chain fatty acid content modulates structure, fluidity, and phase in model microbial cell membranes. *J. Phys. Chem. B* **2019**, *123*, 5814−5821.
(58) Haest, C.W.M.; De Gier, J.; Op Den Kamp, J.A.F.; Bartels, P.; Van Deenen, L.L.M. Changes in permeability of Staphylococcus aureus and derived liposomes with varying lipid composition. *BBA - Biomembr.* **1972**, *255*, 720−733.
(59) Kotra, L. P.; Golemi, D.; Amro, N. A.; Liu, G.-Y.; Mobashery, S. Dynamics of the lipopolysaccharide assembly on the surface of Escherichia coli. *J. Am. Chem. Soc.* **1999**, *121*, 8707−8711.
(60) Lins, R. D.; Straatsma, T. Computer simulation of the rough lipopolysaccharide membrane of Pseudomonas aeruginosa. *Biophys. J.* **2001**, *81*, 1037−1046.
(61) Soares, T. A.; Straatsma, T. Towards simulations of outer membrane proteins in lipopolysaccharide membranes. In *AIP Conference Proceedings*; AIP Publishing, 2007; Vol. *963*, No. 2, pp 1375−1378..
(62) Piggot, T. J.; Holdbrook, D. A.; Khalid, S. Electroporation of the E. coli and S. aureus membranes: molecular dynamics simulations of complex bacterial membranes. *J. Phys. Chem. B* **2011**, *115*, 13381−13388.
(63) Kirschner, K. N.; Lins, R. D.; Maass, A.; Soares, T. A. A glycam-based force field for simulations of lipopolysaccharide membranes: parametrization and validation. *J. Chem. Theory Comput.* **2012**, *8*, 4719−4731.
(64) Wu, E. L.; Engström, O.; Jo, S.; Stuhlsatz, D.; Yeom, M. S.; Klauda, J. B.; Widmalm, G.; Im, W. Molecular dynamics and NMR spectroscopy studies of E. coli lipopolysaccharide structure and dynamics. *Biophys. J.* **2013**, *105*, 1444−1455.
(65) Van Oosten, B.; Harroun, T. A. A MARTINI extension for Pseudomonas aeruginosa PAO1 lipopolysaccharide. *J. Mol. Graph. Model.* **2016**, *63*, 125−133.
(66) Ma, H.; Irudayanathan, F. J.; Jiang, W.; Nangia, S. Simulating Gram-negative bacterial outer membrane: a coarse grain model. *J. Phys. Chem. B* **2015**, *119*, 14668−14682.
(67) Kim, S.; Patel, D. S.; Park, S.; Slusky, J.; Klauda, J. B.; Widmalm, G.; Im, W. Bilayer properties of lipid A from various Gram-negative bacteria. *Biophys. J.* **2016**, *111*, 1750−1760.
(68) Hsu, P.-C.; Jefferies, D.; Khalid, S. Molecular dynamics simulations predict the pathways via which pristine fullerenes penetrate bacterial membranes. *J. Phys. Chem. B* **2016**, *120*, 11170−11179.
(69) Hsu, P.-C.; Samsudin, F.; Shearer, J.; Khalid, S. It is complicated: curvature, diffusion, and lipid sorting within the two membranes of Escherichia coli. *J. Phys. Chem. Lett.* **2017**, *8*, 5513−5518.
(70) Lee, J.; Patel, D. S.; Kucharska, I.; Tamm, L. K.; Im, W. Refinement of OprH-LPS interactions by molecular simulations. *Biophys. J.* **2017**, *112*, 346−355.
(71) Ma, H.; Cummins, D. D.; Edelstein, N. B.; Gomez, J.; Khan, A.; Llewellyn, M. D.; Picudella, T.; Willsey, S. R.; Nangia, S. Modeling diversity in structures of bacterial outer membrane lipids. *J. Chem. Theory Comput.* **2017**, *13*, 811−824.

https://doi.org/10.1021/acs.langmuir.3c03474
Langmuir 2024, 40, 7791−7811

(72) Rice, A.; Wereszczynski, J. Atomistic scale effects of lipopolysaccharide modifications on bacterial outer membrane defenses. *Biophys. J.* **2018**, *114*, 1389−1399.
(73) Lee, J.; Patel, D. S.; Ståhle, J.; Park, S.-J.; Kern, N. R.; Kim, S.; Lee, J.; Cheng, X.; Valvano, M. A.; Holst, O.; et al. CHARMM-GUI membrane builder for complex biological membrane simulations with glycolipids and lipoglycans. *J. Chem. Theory Comput.* **2019**, *15*, 775−786.
(74) Jefferies, D.; Shearer, J.; Khalid, S. Role of O-antigen in response to mechanical stress of the E. coli outer membrane: insights from coarse-grained MD simulations. *J. Phys. Chem. B* **2019**, *123*, 3567−3575.
(75) Kesireddy, A.; Pothula, K. R.; Lee, J.; Patel, D. S.; Pathania, M.; van den Berg, B.; Im, W.; Kleinekathöfer, U. Modeling of specific lipopolysaccharide binding sites on a Gram-negative porin. *J. Phys. Chem. B* **2019**, *123*, 5700−5708.
(76) Boags, A. T.; Samsudin, F.; Khalid, S. Binding From both sides: TolR and full-length OmpA bind and maintain the local structure of the E. coli cell wall. *Structure* **2019**, *27*, 713−724.
(77) Shearer, J.; Jefferies, D.; Khalid, S. Outer Membrane Proteins OmpA, FhuA, OmpF, EstA, BtuB, and OmpX Have Unique Lipopolysaccharide Fingerprints. *J. Chem. Theory Comput.* **2019**, *15*, 2608−2619.
(78) Gao, Y.; Lee, J.; Widmalm, G.; Im, W. Preferred conformations of lipooligosaccharides and oligosaccharides of Moraxella catarrhalis. *Glycobiology* **2020**, *30*, 86−94.
(79) Vaiwala, R.; Ayappa, K. G. Martini-3 Coarse-Grained Models for the Bacterial Lipopolysaccharide Outer Membrane of Escherichia coli. *J. Chem. Theory Comput.* **2024**, *20* (4), 1704−1716.
(80) Vanommeslaeghe, K.; Hatcher, E.; Acharya, C.; Kundu, S.; Zhong, S.; Shim, J.; Darian, E.; Guvench, O.; Lopes, P.; Vorobyov, I.; Mackerell, A. D. CHARMM general force field: A force field for drug-like molecules compatible with the CHARMM all-atom additive biological force fields. *J. Comput. Chem.* **2010**, *31*, 671−690.
(81) Wang, J.; Wolf, R. M.; Caldwell, J. W.; Kollman, P. A.; Case, D. A. Development and testing of a general amber force field. *J. Comput. Chem.* **2004**, *25*, 1157−1174.
(82) Jambeck, J. P.; Lyubartsev, A. P. An extension and further validation of an all-atomistic force field for biological membranes. *J. Chem. Theory Comput.* **2012**, *8*, 2938−2948.
(83) Chiu, S.-W.; Pandit, S. A.; Scott, H.; Jakobsson, E. An improved united atom force field for simulation of mixed lipid bilayers. *J. Phys. Chem. B* **2009**, *113*, 2748−2763.
(84) Marrink, S. J.; Risselada, H. J.; Yefimov, S.; Tieleman, D. P.; De Vries, A. H. The MARTINI force field: coarse grained model for biomolecular simulations. *J. Phys. Chem. B* **2007**, *111*, 7812−7824.
(85) Noid, W. G. Perspective: Coarse-grained models for biomolecular systems. *J. Chem. Phys.* **2013**, *139*, No. 090901.
(86) Alessandri, R.; Souza, P. C.; Thallmair, S.; Melo, M. N.; De Vries, A. H.; Marrink, S. J. Pitfalls of the Martini model. *J. Chem. Theory Comput.* **2019**, *15*, 5448−5460.
(87) Souza, P. C.; et al. Martini 3: a general purpose force field for coarse-grained molecular dynamics. *Nat. Methods* **2021**, *18*, 382−388.
(88) Grünewald, F.; Punt, M. H.; Jefferys, E. E.; Vainikka, P. A.; König, M.; Virtanen, V.; Meyer, T. A.; Pezeshkian, W.; Gormley, A. J.; Karonen, M.; Sansom, M. S. P.; Souza, P. C. T.; Marrink, S. J. Martini 3 Coarse-Grained Force Field for Carbohydrates. *J. Chem. Theory Comput.* **2022**, *18*, 7555−7569.
(89) Lutsyk, V.; Wolski, P.; Plazinski, W. Extending the Martini 3 Coarse-Grained Force Field to Carbohydrates. *J. Chem. Theory Comput.* **2022**, *18*, 5089−5107.
(90) Leive, L. Release of lipopolysaccharide by EDTA treatment of E., coli. *Biochem. Biophys. Res. Commun.* **1965**, *21*, 290−296.
(91) Seydel, U.; Eberstein, W.; Schröder, G.; Brandenburg, K. Electrostatic potential barrier in asymmetric planar lipopolysaccharide/phospholipid bilayers probed with the valinomycin-K+ complex. *Z. Naturforsch., C: J. Biosci.* **1992**, *47*, 757−761.
(92) Brandenburg, K.; Seydel, U. Orientation measurements on membrane systems made from lipopolysaccharides and free lipid A by FT-IR spectroscopy. *Eur. Biophys. J.* **1988**, *16*, 83−94.
(93) Abraham, T.; Schooling, S. R.; Nieh, M.-P.; Kučerka, N.; Beveridge, T. J.; Katsaras, J. Neutron diffraction study of Pseudomonas aeruginosa lipopolysaccharide bilayers. *J. Phys. Chem. B* **2007**, *111*, 2477−2483.
(94) Yesylevskyy, S. O.; Schäfer, L. V.; Sengupta, D.; Marrink, S. J. Polarizable water model for the coarse-grained MARTINI force field. *PLoS Comput. Biol.* **2010**, *6*, No. e1000810.
(95) BRANDENBURG, K.; SEYDEL, U. Investigation into the fluidity of lipopolysaccharide and free lipid A membrane systems by Fourier-transform infrared spectroscopy and differential scanning calorimetry. *Eur. J. Biochem.* **1990**, *191*, 229−236.
(96) Paracini, N.; Clifton, L. A.; Skoda, M. W.; Lakey, J. H. Liquid crystalline bacterial outer membranes are critical for antibiotic susceptibility. *Proc. Natl. Acad. Sci. U.S.A.* **2018**, *115*, E7587−E7594.
(97) Schmalhorst, P. S.; Deluweit, F.; Scherrers, R.; Heisenberg, C.-P.; Sikora, M. Overcoming the limitations of the MARTINI force field in simulations of polysaccharides. *J. Chem. Theory Comput.* **2017**, *13*, 5039−5053.
(98) Shivgan, A. T.; Marzinek, J. K.; Huber, R. G.; Krah, A.; Henchman, R. H.; Matsudaira, P.; Verma, C. S.; Bond, P. J. Extending the Martini coarse-grained force field to N-glycans. *J. Chem. Inf. Model.* **2020**, *60*, 3864−3883.
(99) Carpenter, T. S.; Parkin, J.; Khalid, S. The free energy of small solute permeation through the Escherichia coli outer membrane has a distinctly asymmetric profile. *J. Phys. Chem. Lett.* **2016**, *7*, 3446−3451.
(100) Guo, L.; Lim, K. B.; Gunn, J. S.; Bainbridge, B.; Darveau, R. P.; Hackett, M.; Miller, S. I. Regulation of lipid A modifications by Salmonella typhimurium virulence genes phoP-phoQ. *Science* **1997**, *276*, 250−253.
(101) Luna, E.; Kim, S.; Gao, Y.; Widmalm, G.; Im, W. Influences of Vibrio cholerae lipid A types on LPS bilayer properties. *J. Phys. Chem. B* **2021**, *125*, 2105−2112.
(102) Vergalli, J.; Bodrenko, I. V.; Masi, M.; Moynié, L.; Acosta-Gutíerrez, S.; Naismith, J. H.; Davin-Regli, A.; Ceccarelli, M.; Van den Berg, B.; Winterhalter, M.; et al. Porins and small-molecule translocation across the outer membrane of Gram-negative bacteria. *Nat. Rev. Microbiol.* **2020**, *18*, 164−176.
(103) Benn, G.; Mikheyeva, I. V.; Inns, P. G.; Forster, J. C.; Ojkic, N.; Bortolini, C.; Ryadnov, M. G.; Kleanthous, C.; Silhavy, T. J.; Hoogenboom, B. W. Phase separation in the outer membrane of Escherichia coli. *Proc. Natl. Acad. Sci. U.S.A.* **2021**, *118*, No. e2112237118.
(104) Goose, J. E.; Sansom, M. S. Reduced lateral mobility of lipids and proteins in crowded membranes. *PLoS Comp. Biol.* **2013**, *9*, No. e1003033.
(105) Arunmanee, W.; Pathania, M.; Solovyova, A. S.; Le Brun, A. P.; Ridley, H.; Baslé, A.; van den Berg, B.; Lakey, J. H. Gram-negative trimeric porins have specific LPS binding sites that are essential for porin biogenesis. *Proc. Natl. Acad. Sci. U.S.A.* **2016**, *113*, E5034−E5043.
(106) Pandit, K. R.; Klauda, J. B. Membrane models of E. coli containing cyclic moieties in the aliphatic lipid chain. *BBA-Biomembr.* **2012**, *1818*, 1205−1210.
(107) Hong, C.; Tieleman, D. P.; Wang, Y. Microsecond molecular dynamics simulations of lipid mixing. *Langmuir* **2014**, *30*, 11993−12001.
(108) Kalli, A. C.; Sansom, M. S.; Reithmeier, R. A. Molecular dynamics simulations of the bacterial UraA H+-uracil symporter in lipid bilayers reveal a closed state and a selective interaction with cardiolipin. *PLoS Comput. Biol.* **2015**, *11*, No. e1004123.
(109) Alcock, F.; Stansfeld, P. J.; Basit, H.; Habersetzer, J.; Baker, M. A.; Palmer, T.; Wallace, M. I.; Berks, B. C. Assembling the Tat protein translocase. *eLife* **2016**, *5*, No. e20718.
(110) Jahangiri, S.; Jafari, M.; Arjomand, M.; Mehrnejad, F. Molecular insights into the interactions of GF-17 with the gram-

https://doi.org/10.1021/acs.langmuir.3c03474
Langmuir 2024, 40, 7791−7811

negative and gram-positive bacterial lipid bilayers. *J. Cell. Biochem.* **2018**, *119*, 9205−9216.
(111) Rocha-Roa, C.; Orjuela, J. D.; Leidy, C.; Cossio, P.; Aponte-Santamaría, C. Cardiolipin prevents pore formation in phosphatidylglycerol bacterial membrane models. *FEBS Lett.* **2021**, *595*, 2701−2714.
(112) Sharma, P.; Vaiwala, R.; Parthasarathi, S.; Patil, N.; Verma, A.; Waskar, M.; Raut, J. S.; Basu, J. K.; Ayappa, K. G. Interactions of surfactants with the bacterial cell wall and inner membrane: Revealing the link between aggregation and antimicrobial activity. *Langmuir* **2022**, *38*, 15714−15728.
(113) Vaiwala, R.; Sharma, P.; Puranik, M.; Ayappa, K. G. Developing a Coarse-Grained Model for Bacterial Cell Walls: Evaluating Mechanical Properties and Free Energy Barriers. *J. Chem. Theory Comput.* **2020**, *16*, 5369−5384.
(114) Pink, D.; Moeller, J.; Quinn, B.; Jericho, M.; Beveridge, T. On the architecture of the gram-negative bacterial murein sacculus. *J. Bacteriol.* **2000**, *182*, 5925−5930.
(115) Koch, A. L. Length distribution of the peptidoglycan chains in the sacculus of Escherichia coli. *J. Theor. Biol.* **2000**, *204*, 533−541.
(116) Dmitriev, B. A.; Toukach, F. V.; Schaper, K.-J.; Holst, O.; Rietschel, E. T.; Ehlers, S. Tertiary structure of bacterial murein: the scaffold model. *J. Bacteriol.* **2003**, *185*, 3458−3468.
(117) Dmitriev, B. A.; Toukach, F. V.; Holst, O.; Rietschel, E.; Ehlers, S. Tertiary structure of Staphylococcus aureus cell wall murein. *J. Bacteriol.* **2004**, *186*, 7141−7148.
(118) Samsudin, F.; Ortiz-Suarez, M. L.; Piggot, T. J.; Bond, P. J.; Khalid, S. OmpA: a flexible clamp for bacterial cell wall attachment. *Structure* **2016**, *24*, 2227−2235.
(119) Ortiz-Suarez, M. L.; Samsudin, F.; Piggot, T. J.; Bond, P. J.; Khalid, S. Full-length OmpA: structure, function, and membrane interactions predicted by molecular dynamics simulations. *Biophys. J.* **2016**, *111*, 1692−1702.
(120) Samsudin, F.; Boags, A.; Piggot, T. J.; Khalid, S. Braun's lipoprotein facilitates OmpA interaction with the Escherichia coli cell wall. *Biophys. J.* **2017**, *113*, 1496−1504.
(121) Pushkaran, A. C.; Nataraj, N.; Nair, N.; Götz, F.; Biswas, R.; Mohan, C. G. Understanding the structure−function relationship of lysozyme resistance in Staphylococcus aureus by peptidoglycan O-acetylation using molecular docking, dynamics, and lysis assay. *J. Chem. Inf. Model.* **2015**, *55*, 760−770.
(122) Vaiwala, R.; Sharma, P.; Ganapathy Ayappa, K. Differentiating interactions of antimicrobials with Gram-negative and Gram-positive bacterial cell walls using molecular dynamics simulations. *Biointerphases* **2022**, *17*, 061008.
(123) Witzke, S.; Petersen, M.; Carpenter, T. S.; Khalid, S. Molecular dynamics simulations reveal the conformational flexibility of lipid II and its loose association with the defensin plectasin in the Staphylococcus aureus membrane. *Biochemistry* **2016**, *55*, 3303−3314.
(124) Lins, R. D.; Vorpagel, E. R.; Guglielmi, M.; Straatsma, T. Computer simulation of uranyl uptake by the rough lipopolysaccharide membrane of Pseudomonas aeruginosa. *Biomacromolecules* **2008**, *9*, 29−35.
(125) Orekhov, P. S.; Kholina, E. G.; Bozdaganyan, M. E.; Nesterenko, A. M.; Kovalenko, I. B.; Strakhovskaya, M. G. Molecular mechanism of uptake of cationic Photoantimicrobial Phthalocyanine across bacterial membranes revealed by molecular dynamics simulations. *J. Phys. Chem. B* **2018**, *122*, 3711−3722.
(126) Samsudin, F.; Khalid, S. Movement of Arginine through OprD: The Energetics of Permeation and the Role of Lipopolysaccharide in Directing Arginine to the Protein. *J. Phys. Chem. B* **2019**, *123*, 2824−2832.
(127) Vermaas, J. V.; Crowley, M. F.; Beckham, G. T. Molecular simulation of lignin-related aromatic compound permeation through gram-negative bacterial outer membranes. *J. Biol. Chem.* **2022**, *298*, 102627.
(128) Nikaido, H. Molecular basis of bacterial outer membrane permeability revisited. *Microbiol. Mol. Biol. Rev.* **2003**, *67*, 593−656.
(129) Wiener, M. C.; Horanyi, P. S. How hydrophobic molecules traverse the outer membranes of Gram-negative bacteria. *Proc. Natl. Acad. Sci. U.S.A.* **2011**, *108*, 10929−10930.
(130) Bakry, R.; Vallant, R. M.; Najam-ul Haq, M.; Rainer, M.; Szabo, Z.; Huck, C. W.; Bonn, G. K. Medicinal applications of fullerenes. *Int. J. Nanomed.* **2007**, *2*, 639−649.
(131) Falla, T. J.; Karunaratne, D. N.; Hancock, R. E. Mode of action of the antimicrobial peptide indolicidin. *J. Biol. Chem.* **1996**, *271*, 19298−19303.
(132) Vermaas, J. V.; Dixon, R. A.; Chen, F.; Mansfield, S. D.; Boerjan, W.; Ralph, J.; Crowley, M. F.; Beckham, G. T. Passive membrane transport of lignin-related compounds. *Proc. Natl. Acad. Sci. U.S.A.* **2019**, *116*, 23117−23123.
(133) Bertani, B.; Ruiz, N. Function and biogenesis of lipopolysaccharides. *EcoSal Plus* **2018**, *8* (1), 1.
(134) Watanabe, M.; Rosenbusch, J.; Schirmer, T.; Karplus, M. Computer simulations of the OmpF porin from the outer membrane of Escherichia coli. *Biophys. J.* **1997**, *72*, 2094−2102.
(135) Suenaga, A.; Komeiji, Y.; Uebayasi, M.; Meguro, T.; Saito, M.; Yamato, I. Computational observation of an ion permeation through a channel protein. *Biosci. Rep.* **1998**, *18*, 39−48.
(136) Tieleman, D.; Berendsen, H. A molecular dynamics study of the pores formed by Escherichia coli OmpF porin in a fully hydrated palmitoyloleoylphosphatidylcholine bilayer. *Biophys. J.* **1998**, *74*, 2786−2801.
(137) Im, W.; Roux, B. Ions and counterions in a biological channel: a molecular dynamics simulation of OmpF porin from Escherichia coli in an explicit membrane with 1 M KCl aqueous salt solution. *J. Mol. Biol.* **2002**, *319*, 1177−1197.
(138) Pavlova, A.; Hwang, H.; Lundquist, K.; Balusek, C.; Gumbart, J. C. Living on the edge: Simulations of bacterial outer-membrane proteins. *BBA-Biomembr.* **2016**, *1858*, 1753−1759.
(139) Acharya, A.; Prajapati, J. D.; Kleinekathöfer, U. Improved sampling and free energy estimates for antibiotic permeation through bacterial porins. *J. Chem. Theory and Comp.* **2021**, *17*, 4564−4577.
(140) Bajaj, H.; Acosta Gutierrez, S.; Bodrenko, I.; Malloci, G.; Scorciapino, M. A.; Winterhalter, M.; Ceccarelli, M. Bacterial outer membrane porins as electrostatic nanosieves: exploring transport rules of small polar molecules. *ACS Nano* **2017**, *11*, 5465−5473.
(141) Ceccarelli, M.; Danelon, C.; Laio, A.; Parrinello, M. Microscopic mechanism of antibiotics translocation through a porin. *Biophys. J.* **2004**, *87*, 58−64.
(142) Kumar, A.; Hajjar, E.; Ruggerone, P.; Ceccarelli, M. Molecular simulations reveal the mechanism and the determinants for ampicillin translocation through OmpF. *J. Phys. Chem. B* **2010**, *114*, 9608−9616.
(143) Golla, V. K.; Prajapati, J. D.; Joshi, M.; Kleinekathöfer, U. Exploration of free energy surfaces across a membrane channel using metadynamics and umbrella sampling. *J. Chem. Theory Comput.* **2020**, *16*, 2751−2765.
(144) Wong, J. L.; Romano, M.; Kerry, L. E.; Kwong, H.-S.; Low, W.-W.; Brett, S. J.; Clements, A.; Beis, K.; Frankel, G. OmpK36-mediated Carbapenem resistance attenuates ST258 Klebsiella pneumoniae in vivo. *Nat. Commun.* **2019**, *10*, 3957.
(145) Golla, V. K.; Sans-Serramitjana, E.; Pothula, K. R.; Benier, L.; Bafna, J. A.; Winterhalter, M.; Kleinekathöfer, U. Fosfomycin permeation through the outer membrane porin OmpF. *Biophys. J.* **2019**, *116*, 258−269.
(146) Dai, Y.; Ma, H.; Wu, M.; Welsch, T. A.; Vora, S. R.; Ren, D.; Nangia, S. Development of the computational antibiotic screening platform (CLASP) to aid in the discovery of new antibiotics. *Soft Matter* **2021**, *17*, 2725−2736.
(147) Pedebos, C.; Smith, I. P. S.; Boags, A.; Khalid, S. The hitchhiker's guide to the periplasm: Unexpected molecular interactions of polymyxin B1 in E. coli. *Structure* **2021**, *29*, 444−456.
(148) Jia, Z.; O'Mara, M. L.; Zuegg, J.; Cooper, M. A.; Mark, A. E. The effect of environment on the recognition and binding of vancomycin to native and resistant forms of lipid II. *Biophys. J.* **2011**, *101*, 2684−2692.

https://doi.org/10.1021/acs.langmuir.3c03474
Langmuir 2024, 40, 7791−7811

(149) Ślusarz, R.; Szulc, M.; Madaj, J. Molecular modeling of Gram-positive bacteria peptidoglycan layer, selected glycopeptide antibiotics and vancomycin derivatives modified with sugar moieties. *Carbohydr. Res.* **2014**, *389*, 154−164.
(150) Ślusarz, R.; Ślusarz, M.; Samaszko, J.; Madaj, J. Conformational changes of peptidoglycan fragments during their interactions with vancomycin. *Open Chem.* **2011**, *9*, 422−431.
(151) Olademehin, O. P.; Kim, S. J.; Shuford, K. L. Molecular dynamics simulation of atomic interactions in the vancomycin binding site. *ACS omega* **2021**, *6*, 775−785.
(152) Falk, N. A. Surfactants as Antimicrobials: A Brief Overview of Microbial Interfacial Chemistry and Surfactant Antimicrobial Activity. *J. Surfactants Deterg.* **2019**, *22*, 1119−1127.
(153) Heerklotz, H. Interactions of surfactants with lipid membranes. *Q. Rev. Biophys.* **2008**, *41*, 205.
(154) Pizzirusso, A.; De Nicola, A.; Sevink, G. A.; Correa, A.; Cascella, M.; Kawakatsu, T.; Rocco, M.; Zhao, Y.; Celino, M.; Milano, G. Biomembrane solubilization mechanism by Triton X-100: a computational study of the three stage model. *Phys. Chem. Chem. Phys.* **2017**, *19*, 29780−29794.
(155) Helenius, A.; Simons, K. Solubilization of membranes by detergents. *BBA)-Rev. Biomembr.* **1975**, *415*, 29−79.
(156) Xu, B.; Lin, W.-Q.; Wang, X.-G.; Zeng, S.-w.; Zhou, G.-Q.; Chen, J.-L. Molecular dynamics simulations of the effects of sodium dodecyl sulfate on lipid bilayer. *Chinese Physics B* **2017**, *26*, No. 033103.
(157) Schneider, M. J.; Feller, S. E. Molecular Dynamics Simulations of a Phospholipid- Detergent Mixture. *J. Phys. Chem. B* **2001**, *105*, 1331−1337.
(158) Bandyopadhyay, S.; Shelley, J. C.; Klein, M. L. Molecular dynamics study of the effect of surfactant on a biomembrane. *J. Phys. Chem. B* **2001**, *105*, 5979−5986.
(159) Groot, R. D.; Rabone, K. Mesoscopic simulation of cell membrane damage, morphology change and rupture by nonionic surfactants. *Biophys. J.* **2001**, *81*, 725−736.
(160) Groot, R. D.; Warren, P. B. Dissipative particle dynamics: Bridging the gap between atomistic and mesoscopic simulation. *J. Chem. Phys.* **1997**, *107*, 4423−4435.
(161) Huang, K.-C.; Lin, C.-M.; Tsao, H.-K.; Sheng, Y.-J. The interactions between surfactants and vesicles: Dissipative particle dynamics. *J. Chem. Phys.* **2009**, *130*, No. 245101.
(162) Lin, C.-M.; Chang, G.-P.; Tsao, H.-K.; Sheng, Y.-J. Solubilization mechanism of vesicles by surfactants: effect of hydrophobicity. *J. Chem. Phys.* **2011**, *135*, No. 045102.
(163) Pizzirusso, A.; De Nicola, A.; Milano, G. MARTINI coarse-grained model of Triton TX-100 in pure DPPC monolayer and bilayer interfaces. *J. Phys. Chem. B* **2016**, *120*, 3821−3832.
(164) Schott, H. Comparing the surface chemical properties and the effect of salts on the cloud point of a conventional nonionic surfactant, octoxynol 9 (Triton X-100), and of its oligomer, tyloxapol (Triton WR-1339). *J. Colloid Interface Sci.* **1998**, *205*, 496−502.
(165) Aronica, P. G.; Reid, L. M.; Desai, N.; Li, J.; Fox, S. J.; Yadahalli, S.; Essex, J. W.; Verma, C. S. Computational methods and tools in antimicrobial peptide research. *J. Chem. Inf. Model.* **2021**, *61*, 3172−3196.
(166) Amos, S.-B. T. A.; Vermeer, L. S.; Ferguson, P. M.; Kozlowska, J.; Davy, M.; Bui, T. T.; Drake, A. F.; Lorenz, C. D.; Mason, A. J. Antimicrobial peptide potency is facilitated by greater conformational flexibility when binding to gram-negative bacterial inner membranes. *Sci. Rep.* **2016**, *6*, No. 37639.
(167) Sancho-Vaello, E.; Gil-Carton, D.; François, P.; Bonetti, E.-J.; Kreir, M.; Pothula, K. R.; Kleinekathöfer, U.; Zeth, K. The structure of the antimicrobial human cathelicidin LL-37 shows oligomerization and channel formation in the presence of membrane mimics. *Sci. Rep.* **2020**, *10*, No. 17356.
(168) Wang, Y.; Schlamadinger, D. E.; Kim, J. E.; McCammon, J. A. Comparative molecular dynamics simulations of the antimicrobial peptide CM15 in model lipid bilayers. *BBA-Biomembr.* **2012**, *1818*, 1402−1409.
(169) Bennett, W. D.; Hong, C. K.; Wang, Y.; Tieleman, D. P. Antimicrobial peptide simulations and the influence of force field on the free energy for pore formation in lipid bilayers. *J. Chem. Theory Comput.* **2016**, *12*, 4524−4533.
(170) Bennett, A. L.; Cranford, K. N.; Bates, A. L.; Sabatini, C. R.; Lee, H.-S. A molecular dynamics study of cell-penetrating peptide transportan-10 (TP10): Binding, folding and insertion to transmembrane state in zwitterionic membrane. *Biochim. Biophys. Acta, Biomembr.* **2024**, *1866*, No. 184218.
(171) Balatti, G. E.; Martini, M. F.; Pickholz, M. A coarse-grained approach to studying the interactions of the antimicrobial peptides aurein 1.2 and maculatin 1.1 with POPG/POPE lipid mixtures. *J. Mol. Model.* **2018**, *24*, 208.
(172) Losasso, V.; Agarwal, K.; Waskar, M.; Majumdar, A.; Crain, J.; Winn, M.; Hoptroff, M. Small molecules enhance the potency of natural antimicrobial peptides. *Biophys. J.* **2022**, *121*, 491−501.
(173) Wang, G. Determination of solution structure and lipid micelle location of an engineered membrane peptide by using one NMR experiment and one sample. *Biochim. Biophys. Acta, Biomembr.* **2007**, *1768*, 3271−3281.
(174) Wang, G.; Mishra, B.; Epand, R. F.; Epand, R. M. High-quality 3D structures shine light on antibacterial, anti-biofilm and antiviral activities of human cathelicidin LL-37 and its fragments. *Biochimica et Biophysica Acta (BBA)-Biomembranes* **2014**, *1838*, 2160−2172.
(175) Wang, G.; Epand, R. F.; Mishra, B.; Lushnikova, T.; Thomas, V. C.; Bayles, K. W.; Epand, R. M. Decoding the functional roles of cationic side chains of the major antimicrobial region of human cathelicidin LL-37. *Antimicrob. Agents Chemother.* **2012**, *56*, 845−856.
(176) Aghazadeh, H.; Ganjali Koli, M.; Ranjbar, R.; Pooshang Bagheri, K. Interactions of GF-17 derived from LL-37 antimicrobial peptide with bacterial membranes: a molecular dynamics simulation study. *J. Comput. Aided Mol. Des.* **2020**, *34*, 1261−1273.
(177) Zou, R.; Zhu, X.; Tu, Y.; Wu, J.; Landry, M. P. Activity of antimicrobial peptide aggregates decreases with increased cell membrane embedding free energy cost. *Biochemistry* **2018**, *57*, 2606−2610.
(178) Liu, B.; Karttunen, M. Lipopeptide daptomycin: Interactions with bacterial and phospholipid membranes, stability of membrane aggregates and micellation in solution. *BBA-Biomembr.* **2018**, *1860*, 1949−1954.
(179) Poger, D.; Poyry, S.; Mark, A. E. Could cardiolipin protect membranes against the action of certain antimicrobial peptides? Aurein 1.2, a case study. *ACS omega* **2018**, *3*, 16453−16464.
(180) Berglund, N. A.; Piggot, T. J.; Jefferies, D.; Sessions, R. B.; Bond, P. J.; Khalid, S. Interaction of the antimicrobial peptide polymyxin B1 with both membranes of E. coli: a molecular dynamics study. *PLoS Comput. Biol.* **2015**, *11*, No. e1004180.
(181) Jefferies, D.; Hsu, P.-C.; Khalid, S. Through the lipopolysaccharide glass: a potent antimicrobial peptide induces phase changes in membranes. *Biochemistry* **2017**, *56*, 1672−1679.
(182) Santos, D. E.; Pol-Fachin, L.; Lins, R. D.; Soares, T. A. Polymyxin binding to the bacterial outer membrane reveals cation displacement and increasing membrane curvature in susceptible but not in resistant lipopolysaccharide chemotypes. *J. Chem. Inf. Model.* **2017**, *57*, 2181−2193.
(183) Jiang, X.; Han, M.; Tran, K.; Patil, N. A.; Ma, W.; Roberts, K. D.; Xiao, M.; Sommer, B.; Schreiber, F.; Wang, L.; et al. An Intelligent Strategy with All-Atom Molecular Dynamics Simulations for the Design of Lipopeptides against Multidrug-Resistant Pseudomonas aeruginosa. *J. Med. Chem.* **2022**, *65*, 10001−10013.
(184) Maleš, M.; Zoranić, L. Simulation Study of the Effect of Antimicrobial Peptide Associations on the Mechanism of Action with Bacterial and Eukaryotic Membranes. *Membr.* **2022**, *12*, 891.
(185) Kim, H.; Yoo, Y. D.; Lee, G. Y. Identification of bacterial membrane selectivity of Romo1-derived antimicrobial peptide AMPR-22 via molecular dynamics. *Int. J. Mol. Sci.* **2022**, *23*, 7404.
(186) Sharma, P.; Ayappa, K. G. A molecular dynamics study of antimicrobial peptide interactions with the lipopolysaccharides of the outer bacterial membrane. *J. Membr. Biol.* **2022**, *255*, 665−675.

https://doi.org/10.1021/acs.langmuir.3c03474
Langmuir 2024, 40, 7791−7811

(187) Kulshrestha, A.; Punnathanam, S. N.; Roy, R.; Ayappa, K. G. Cholesterol catalyzes unfolding in membrane-inserted motifs of the pore forming protein cytolysin A. *Biophys. J.* **2023**, *122*, 4068−4081.
(188) Khalid, S.; Schroeder, C.; Bond, P. J.; Duncan, A. L. What have molecular simulations contributed to understanding of Gram-negative bacterial cell envelopes? *Microbiol* **2022**, *168*, No. 001165.
(189) Athar, M.; Gervasoni, S.; Catte, A.; Basciu, A.; Malloci, G.; Ruggerone, P.; Vargiu, A. V. Tripartite efflux pumps of the RND superfamily: what did we learn from computational studies? *Microbiology* **2023**, *169*, No. 001307.
(190) Mitsuta, Y.; Asada, T.; Shigeta, Y. Calculation of the permeability coefficients of small molecules through lipid bilayers by free-energy reaction network analysis following the explicit treatment of the internal conformation of the solute. *Phys. Chem. Chem. Phys.* **2022**, *24*, 26070−26082.
(191) Kmiecik, S.; Gront, D.; Kolinski, M.; Wieteska, L.; Dawid, A. E.; Kolinski, A. Coarse-grained protein models and their applications. *Chem. Rev.* **2016**, *116*, 7898−7936.
(192) Svirina, A.; Chamachi, N.; Schlierf, M. Single-molecule approaches reveal outer membrane protein biogenesis dynamics. *BioEssays* **2022**, *44*, No. 2200149.

https://doi.org/10.1021/acs.langmuir.3c03474
Langmuir 2024, 40, 7791−7811